1994-09

A need to calibrate indicator for high frequency direction finding systems

Partsalidis, Ioannis

Monterey, California. Naval Postgraduate School

Approved for public release; distribution is unlimited.

A NEED TO CALIBRATE INDICATOR FOR HIGH FREQUENCY DIRECTION FINDING SYSTEMS

by
Ioannis Partsalidis
Lieutenant J.G., Hellenic Navy
B.S., Hellenic Naval Academy, 1987

Submitted in partial fulfillment
of the requirements for the degree of

MASTER OF SCIENCE IN SYSTEMS ENGINEERING
(ELECTRONIC WARFARE)

from the

REPORT DOCUMENTATION PAGE	Form Approved OMB No. 0704

1. AGENCY USE ONLY *(Leave blank)*	2. REPORT DATE September , 1994	3. REPORT TYPE AND DATES COVERED Master's Thesis, Final

4. TITLE AND SUBTITLE A NEED TO CALIBRATE INDICATOR FOR HIGH FREQUENCY DIRECTION FINDING SYSTEMS.	5. FUNDING NUMBERS
6. AUTHOR(S) Partsalidis, Ioannis	
7. PERFORMING ORGANIZATION NAME(S) AND ADDRESS(ES) Naval Postgraduate School Monterey CA 93943-5000	8. PERFORMING ORGANIZATION REPORT NUMBER
9. SPONSORING/MONITORING AGENCY NAME(S) AND ADDRESS(ES)	10. SPONSORING/MONITORING AGENCY REPORT NUMBER

11. SUPPLEMENTARY NOTES The views expressed in this thesis are those of the author and do not reflect the official policy or position of the Department of Defense or the U.S. Government.

12a. DISTRIBUTION/AVAILABILITY STATEMENT Approved for public release; distribution unlimited	12b. DISTRIBUTION CODE

13. ABSTRACT

This thesis proposes and investigates a new approach in attacking the "need to calibrate" problem of the shipboard HFDF systems. It is based on measuring the system response to multiple onboard near-field sources. The test is performed along with the standard calibration, and the antenna responses to the near-field sources are stored in a reference database. Whenever a modification is made to the toposide, the near-field test is repeated and the new results are compared to the near-field reference database. A significant difference may indicate a need to perform a full system calibration. The calibration procedure was simulated using the numerical electromagnetics code PATCH. Calculations show that the antenna responses are comparable when topside changes were introduced.

14. SUBJECT TERMS Calibration, HFDF, Classic Outboard, Combat DF.	15. NUMBER OF PAGES 65
	16. PRICE CODE

17. SECURITY CLASSIFICATION OF REPORT	18. SECURITY CLASSIFICATION OF THIS PAGE	19. SECURITY CLASSIFICATION OF ABSTRACT	20. LIMITATION OF ABSTRACT
Unclassified	Unclassified	Unclassified	UL

NSN 7540-01-280-5500

Standard Form 298 (Rev. 2-89)
Prescribed by ANSI Std. 239-18

ABSTRACT

This thesis proposes and investigates a new approach in attacking the "need to calibrate" problem of the shipboard HFDF systems. It is based on measuring the system response to multiple onboard near-field sources. The test is performed along with the standard calibration, and the antenna responses to the near-field sources are stored in a reference database. Whenever a modification is made to the topside, the near-field test is repeated and the new results are compared to the near-field reference database. A significant difference may indicate a need to perform a full system calibration. The calibration procedure was simulated using the numerical electromagnetics code PATCH. Calculations show that the antenna responses for near and far-field sources are comparable when topside changes were introduced.

TABLE OF CONTENTS

ACKNOWLEDGMENT

I would like to express my graditude to the Hellenic Navy for offering me the opportunity to study at such a fine institution as the Naval Postgraduate School. Also, my sincere gratitude and deepest appreciation are due to my thesis advisor, Prof. David Jenn, who triggered my interest on the subject of electromagnetics and showed me that "electromagnetics can be fun." In addition, special thanks are due to Randy Ott, SWL, for providing me with the database of the model. And last, but not least, sincere recognition is due to my wife Louana whose patience and ecouragement helped me through the hard working days.

I. INTRODUCTION

"Thalassocracy" is a word introduced to Western civilization by its earliest historians whose works survive, Herodotus and Thoucydides. "Thalassa," in Greek, means the "sea." To these men and their contemporaries, thalassocracy was a concept which meant, loosely, "maritime supremacy," i.e., the control of the sea lanes and islands by one state to insure its territorial integrity and thus its economical prosperity. "Thalassocracy," therefore, is a universal concept, with technology being the corner stone. Technology has been a driving force in defense since the man threw the first stone thousands of centuries ago. As weapon systems advance in complexity, effectiveness, and in the ability to evade countermeasures, the user demands more of the early warning detection and location systems that support their efforts.

Electronic warfare (EW) is a distinct and well-defined major function in naval operations. In its broadest sense, EW encompasses the employment of all devices and equipment that radiate or receive electromagnetic energy. The inherent weakness of an electromagnetic signal is its susceptibility to detection and interference because of its free-space propagation characteristics. It is the exploitation of this weakness which accounts for a major expenditure of effort in the electronic warfare arena.

Of particular interest in this thesis is the field of tactical radio direction finding for early warning and position location of targets. High frequency direction finding (HFDF) has been widely used since World War II. Tactical commanders at sea had their first look at the utility of HFDF during the battle of the Atlantic. HFDF stations were able to provide relatively accurate locations of German U-boats, enabling seaborne units to successfully intercept the submarines. HFDF was eventually installed on board naval surface ships. With the advent of cruise missiles and the need for over the horizon targeting (OTHT), shipboard HFDF was seen as a means of obtaining targeting information without divulging one's own position. Passive signal intelligence offers the tactical commander a viewpoint into the intentions of his adversaries; HFDF further enhances battlefield effectiveness by providing knowledge of the enemy's location.

One of the basic steps in the development of an HFDF system, or any other system, is the determination of the calibration method needed to ensure its operation within the limits set by either the manufacturer or the user. The scope of this thesis is to investigate a method of evaluating the response of the antenna elements of such a system, both before and after modifications to the ship, thus providing an indication of the need to calibrate. This method is based on the excitation of the system to multiple near-field sources, and will subsequently be referred to as the "near-field test method."

Chapter II is an overview of HFDF systems and their capabilities. In addition, the Classic Outboard and Combat DF systems, the associated hardware, and their operation are briefly described.

In Chapter III the present method of calibrating antenna systems and its applicability to the HFDF systems are discussed. This method requires that the ship circle a transmitter while the system response is measured. Currently there is no reliable indicator as to whether a topside modification will affect the system DF accuracy. Therefore, the system is recalibrated after any significant modification. This approach is effective but very costly and time consuming.

In Chapter IV the proposed near-field measurement approach is described and simulated using the electromagnetic code PATCH. A numerical model of the DD 963 (Spruance Class Destroyer) is used to compute the deck-edge antenna response to a range of near-field sources. It is shown that the responses are sensitive to topside modifications if a complete set of transmit locations is considered.

Finally, in Chapter V, the data is summarized and conclusions and recommendations for future work are presented.

II. OVERVIEW OF HFDF METHODS

A. HIGH FREQUENCY DIRECTION FINDING (HFDF)

Determining the location of a remote transmitter is important to the Navy in search and rescue, in forecasting the actions and intentions of a potential enemy, and in targeting "fire-and-forget" missiles. There are several methods for deriving geolocation information at HF, and various algorithms attempt to exploit attributes of the schemes. Multiple sites can be used to take advantage of the signal time-difference-of-arrival (TDOA) or bearing angle-of-arrival (AOA). Perhaps the most versatile class of methods are those in the category of the single-station-location (SSL) such as the Classic Outboard and Combat DF systems. SSL refers to methods by which a signal source is located from information at a single receiving site such as a ship. Clearly this requires that some information or assumptions about the propagation path through the ionosphere (sky wave) and over the earth's surface (ground wave).

A HFDF system serves several purposes:

1. integrate shipboard tactical location intelligence with longer range, shore-generated bearing information,
2. exploit the strength of the system while avoiding its weaknesses, and
3. provide this location information in a timely manner to users.

Position location of high frequency radio transmitters consists of three sequential operations:

1. detection of the signal,

2. determination of the direction of emitter (DOE), and

3. computation of the position estimate.

Errors and inaccuracies can be introduced during any of these operations, and if left uncorrected will result in position estimates with little tactical value. The remainder of this section will briefly explain how errors are introduced in each phase of position locating.

The first phase, detection of an HF radio transmitter, is usually thought of as a binary operation: it either occurs or does not occur. However, under certain signal-to-noise (S/N) conditions detection may seem to have occurred when in fact it hasn't, or it may not have occurred when in fact it has. This contradiction is caused primarily by two factors: noise and high signal density (interference). The lack of an observed detection when in fact the radio signal is present is normally caused by noise at the HFDF site. The noise can be self-generated at the site or come from outside sources that cause interference.

The detection of a radio signal at the frequency of interest does not guarantee that the transmitter of interest was detected. The HF spectrum is crowded with multiple users employing the similar signals on the same or near to the same frequency. Multiple HFDF sites may report detections on a frequency and

in fact not be hearing the same transmitter. Detection errors are most likely to occur when there does not exist an HF propagation path between the transmitter of interest and one or more HFDF sites.

The second phase of position location is determination of the direction of emitter (DOE). DOE is defined as the azimuth angle from the HFDF site in the direction of the transmitter of interest. After detection, the HFDF site reports the direction-of-arrival (DOA) of the transmitted signal. When the reported DOA differs from the true DOE an error has been introduced. The true direction of the transmitter is never known precisely in practice, and thus only an estimate exists (which will be referred to as bearing).

Large bearing errors are usually the result of detection errors; smaller more insidious bearing errors are the result of a variety of factors. The most prevalent is the error caused by propagation irregularities. Long range HF communication is made possible by the ionospheric layers which act as reflecting mediums propagating HF signals around the curvature of the earth as shown in Figure 1.

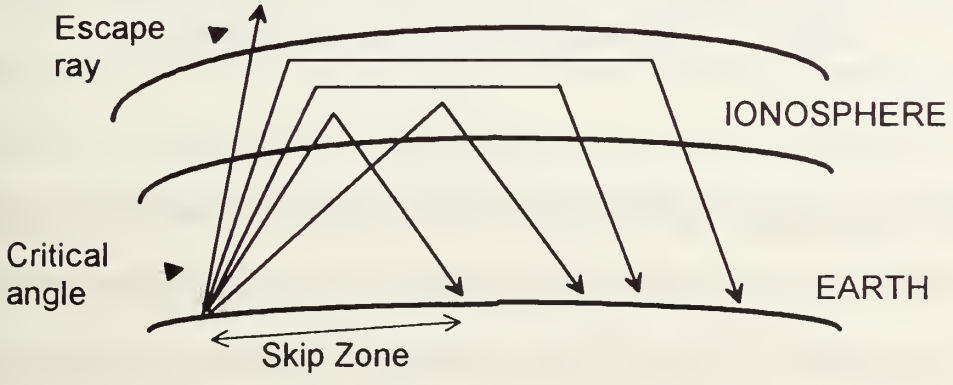

Figure 1. Simplified HF path geometry.

The ionospheric layers are not true reflectors, but are instead refractors that bend the signal back in the direction of the earth's surface as shown in Figure 2. As the signal is refracted the wavefront can be distorted away from its direction of propagation prior to refraction. (The plane defined by the transmitter, receiver, and reflection points illustrated in Figure 2 may not contain the earth's center.) The magnitude of the distortion will determine the degree of the bearing error.

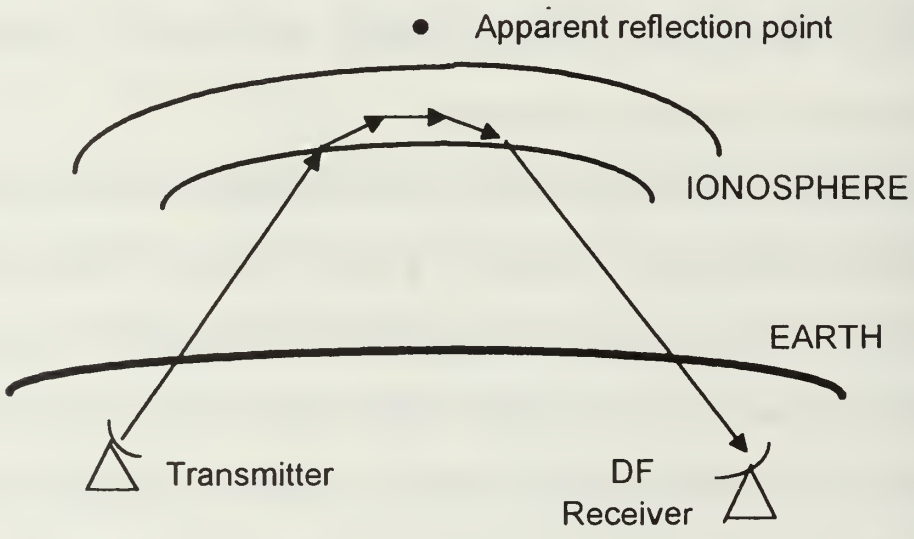

Figure 2. Virtual height of an ionospheric reflection .

Bearings can also be different than the true DOE if reflecting and scattering objects exist in the vicinity of the HFDF antenna. Site errors can be reduced with careful site selection and empirically developed corrections (background subtraction methods).

The final stage of the position locating problem is the actual computation of a position estimate or "fix." In the absence of errors, the position estimate and the transmitter of interest are collocated and for a single station can be determined by phase and time-of-arrival differences between adjacent antennas.

Fix algorithms have been developed to solve the estimation problem with a variety of mathematical techniques. Ideally, the fix algorithm must be capable of

1. differentiating good bearings from bad,
2. adjusting good bearings to correct for small bearing errors, and
3. providing an indication of the estimates accuracy.

B. OVERVIEW OF CLASSIC OUTBOARD AND COMBAT DF SYSTEMS

The Classic Outboard and the Combat DF systems are installed on most Spruance class destroyers (DD 963) as an integral part of their EW capability. A block diagram of Classic Outboard is shown in Figure 3.

Both of these systems employ an array of shielded half-loop antennas with ferrite cores (Figure 4). There are a total of 24 antennas mounted on the surface of the ship and spaced around the perimeter of the deck as shown in Figure 5. They operate from 4 to 30 MHz and are referred to as "deck-edge antennas."

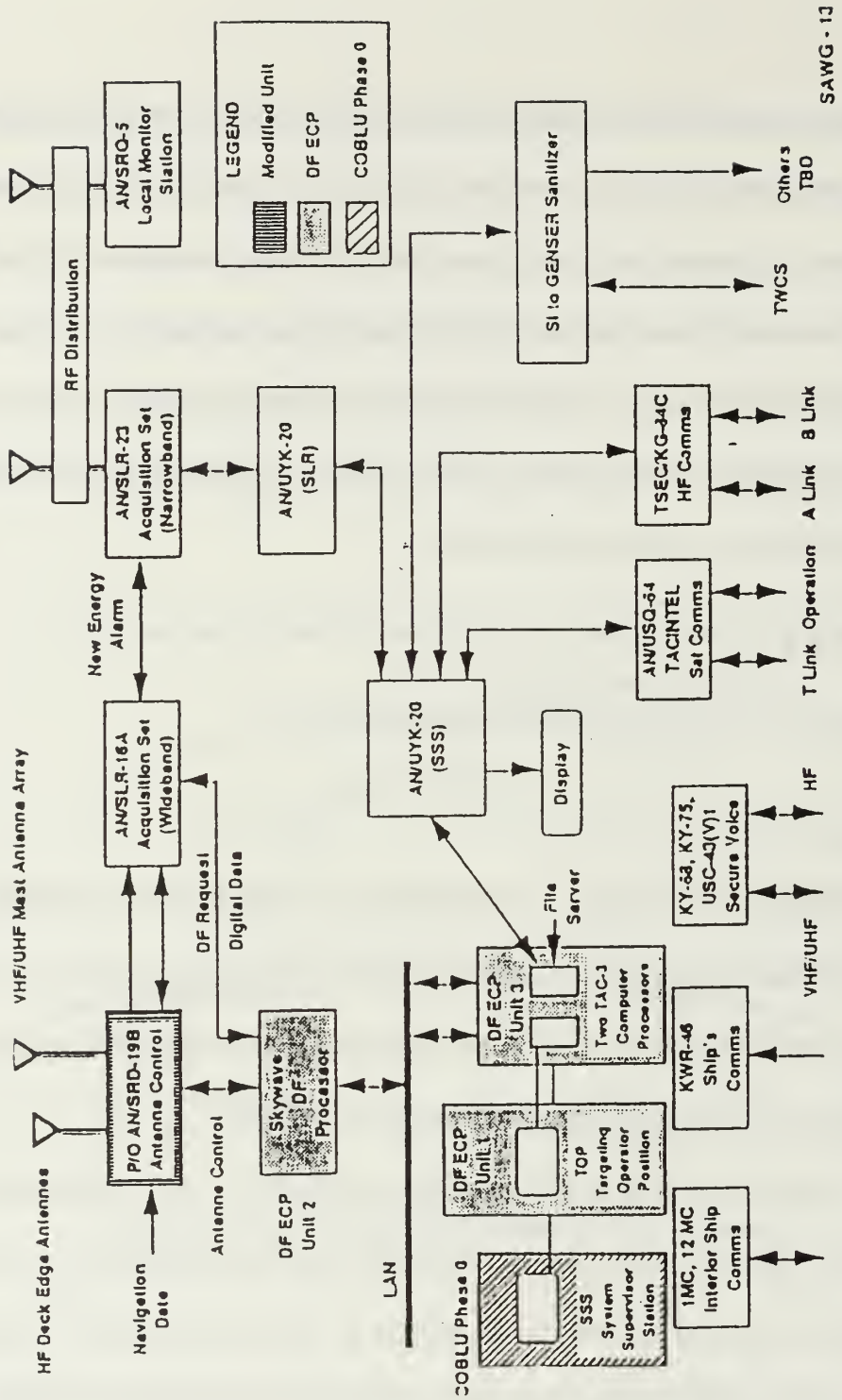

Figure 3. Block diagram of the Classic Outboard System.

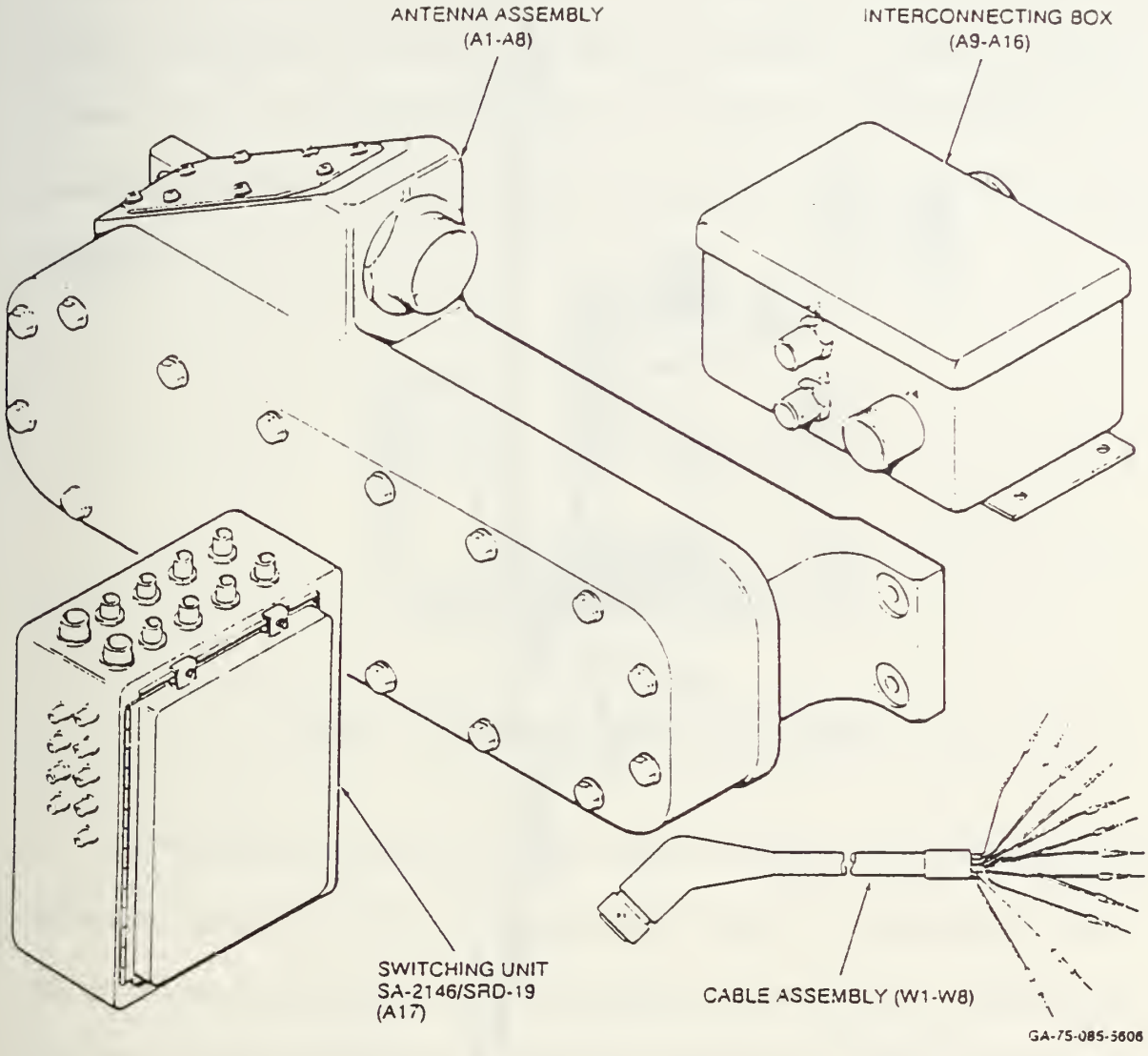

Figure 4. Ferrite loaded loop antenna.

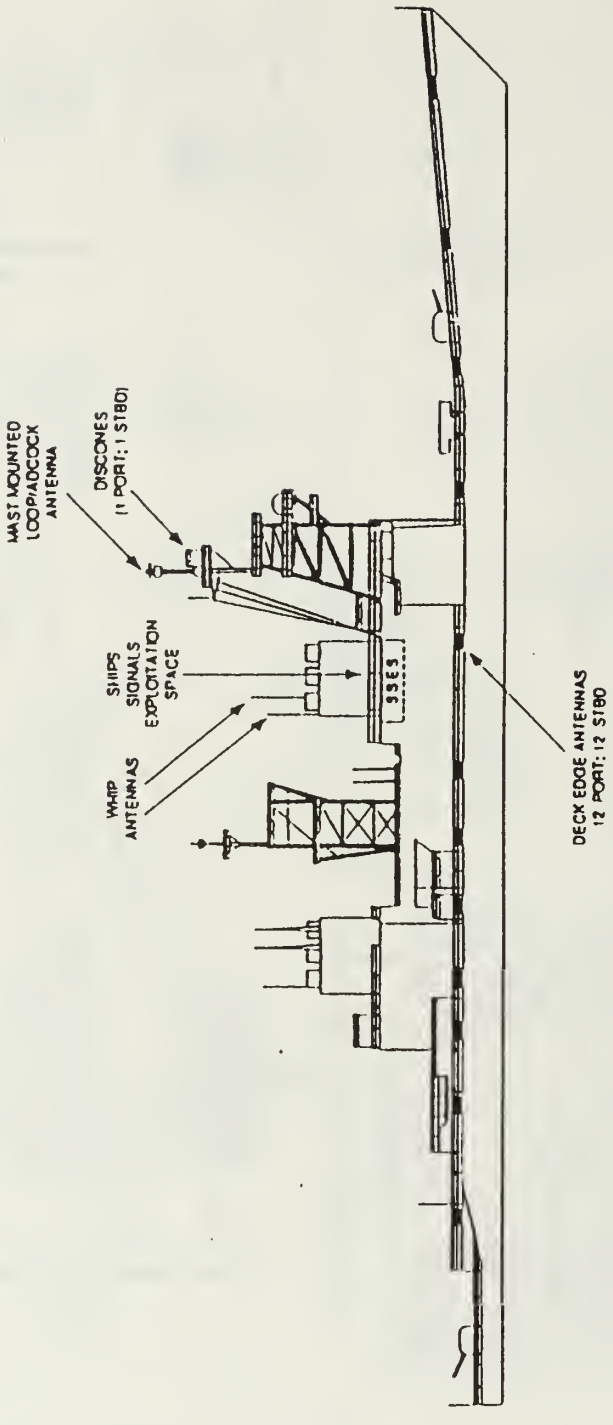

Figure 5. Antennas locations on the ship.

1. Deck-edge Antennas

These deck-edge antennas are attached horizontally (in most cases) directly to the skin of the ship as shown in Figure 6. They serve as current probes that sense the vertical component of the current induced on the ship's surface. This current is primarily due to a vertically polarized incident plane wave, but can also be induced by horizontally polarized waves due to ship scattering.

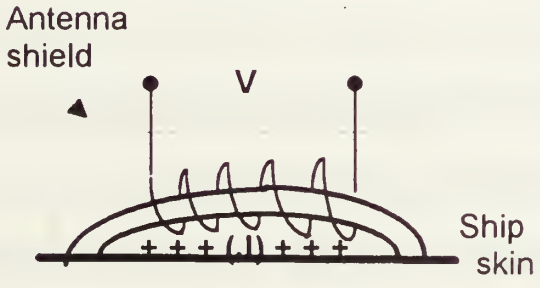

Figure 6. Ferrite loop on the ship's surface.

Current probes (sensors) have been used for many years in different areas of technology [Ref.1]. They are devices which convert an electromagnetic quantity of interest into a voltage or current at some terminal points. A design procedure introduced by Pettengill, et al [Ref. 2] provides an equation which relates the minimum required volume and the optimum dimensions for a fully wound ferrite loaded receiving antenna within the range of 0.5 to 30 MHz

$$W = \frac{18.6\times10^{-4} kTBF_R \mu_0}{E_{min}^2 f^{0.69} \mu_F}\left(\frac{S}{N}\right) \qquad (1)$$

where,

W = antenna volume

k = Boltzman constant

T = absolute temperature

μ_0 = air permeability

f = operating frequency

F_R = receiver noise factor

B = bandwidth

E_{min} = minimum induced emf

μ_F = ferrite core permeability

S/N = signal-to-noise ratio

The important feature of this equation is that the signal-to-noise ratio (SNR) is roughly proportional to the operating frequency.

The probe is calibrated by the manufacturer during production by simply passing a current of known magnitude and frequency through the probe and measuring the voltage at its terminals. The result is a set of calibration curves that relate the voltage (V) to the current (I) and the transfer impedance (the ratio Z=V/I).

2. Direction Finding Algorithm

Outboard and Combat DF incorporate several techniques in order to reduce the error in the bearing measurement. One is to use widely dispersed antenna locations around the perimeter of the ship, thus providing a wider aperture for phase measurement. The exact placement of the antennas is determined

empirically to minimize the interactions and interference from objects and structures on the ship.

Secondly, rather than using an additive or subtractive approach to finding the DOA, the emitter direction is isolated using a technique called correlation interferometer direction finding (CIDF) . The direction is obtained using two sets of data. One consists of the phase and amplitude voltages which result from a known transmitter at a given frequency and relative bearing. This is referred to as the "reference set," and its measurement process as "calibration." The second set consists of phase and amplitude voltage measurements received by each of the antenna array elements from the HF signal of unknown azimuth (the "measurement set"). The azimuth at which maximum correlation between the two sets of data occurs is taken to be the DOA of the incoming signal.

The degree by which the measured antenna voltages matches each of the test voltages is called the complex correlation coefficient (C) and is computed by the formula [Ref. 3]

$$C = \frac{\sum_{n=1}^{N} [U_n(\phi_i) \bullet V_n^*(\phi_t)]}{\sqrt{\sum_{n=1}^{N} |U_n(\phi_i)|^2} \bullet \sqrt{\sum_{n=1}^{N} |V_n(\phi_t)|^2}} \qquad (2)$$

where,

$U_n(\phi_i)$ = complex measured voltage for antenna n,

$V_n(\phi_t)$ = complex stored voltage for antenna n,

ϕ_i = radiation angle of incidence,

ϕ_t = angle of stored voltage set,

and the asterisk denotes complex conjugate. Note that C is normalized so that $0 \leq C \leq 1$. For Classic Outboard, only vertically polarized transmissions are stored, while the Combat DF system uses both vertically and horizontally polarized transmissions to develop the reference database.

To obtain a DOA, the phases and amplitudes of an unknown transmission are measured, and the resulting set of measurements is compared with the stored patterns for best fit. The closest angle-of-arrival estimate is taken as the one with the highest C value by polynomial interpolation, as illustrated in Figure 7 .

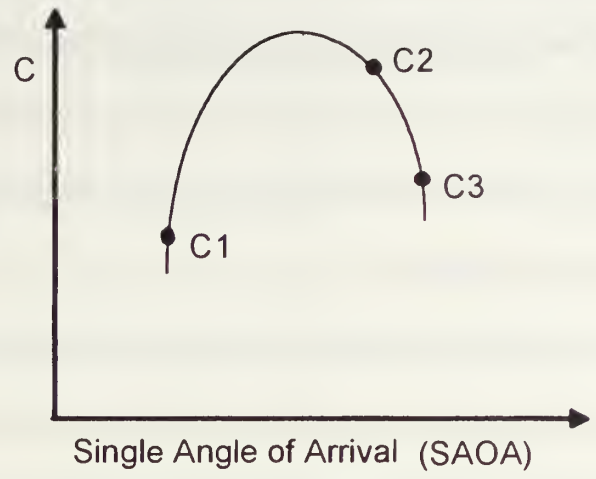

Figure 7. Polynomial interpolation to find SAOA.

The appeal of the CIDF technique is that shipboard scattering effects are automatically included, at least in principle. If a plane wave is incident from the direction ϕ_i , then it should excite the exact same set of voltages as the reference signal from the same direction. Thus $\phi_t = \phi_i$ and C=1. In practice, $\phi_t = \phi_i$ does not always result in perfect correlation because of environmental differences between the operational measurement and the baseline measurement. In other words, propagation conditions are variable due to ocean and ionospheric conditions. These cannot be controlled and therefore always introduce some uncertainty into the DOA measurement.

In addition to environmental variations, any significant change to the ship between calibration and measurement will also affect accuracy. Precisely which change is significant depends on the angle of arrival of the signal and the location of the change. Clearly, a minor change at the bow will not affect antenna

responses astern, but can certainly affect forward antenna performance. The net effect on DOA estimation depends on the relative importance of each antenna's response in computing C. For instance, if the magnitude of an antenna's complex voltage is small relative to other antennas, then large phase errors will have little effect on the DOA estimate.

The "need to calibrate" procedure introduced in Chapter III is a means of evaluating the accuracy of the calibration data-base after a modification is performed on the topside. Thus, it provides a solid criterion to decide whether a need for full-scale calibration of the system exists.

III. CALIBRATION METHOD

A. PRESENT METHOD OF CALIBRATION

One of the basic steps in developing and maintaining a HFDF system is its calibration and performance evaluation. The present method of calibrating HFDF shipboard systems is to circle the ship about an anchored buoy while monitoring signals from a shore site as depicted in Figure 8.

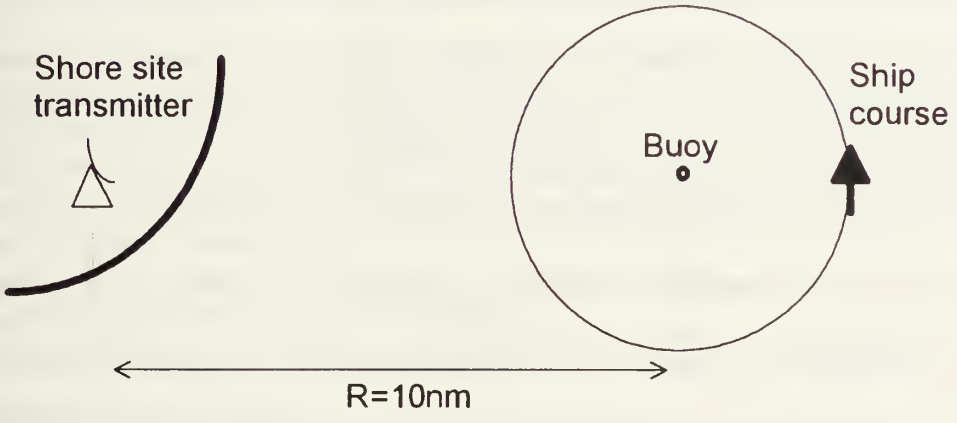

Figure 8. Calibration geometry.

The procedure requires that the ship circle offshore while a transmitter frequency sweeps over the band of interest. At a discrete set of frequencies the DF system response is recorded along with the ship's bearing. Together they completely provide the reference voltage set $V(\phi_i)$. However, because of ship

pitch and roll and the fact that the course is not always circular, the apparent ϕ_t is slightly different than the actual value.

A complete calibration requires several days and as a consequence is very expensive. Currently the calibration is repeated after every "significant" modification, with significant being determined by intuition and past experience. The method proposed in the next section attempts to quantify the need to calibrate.

B. THE PROPOSED METHOD

This thesis proposes and investigates a new approach in attacking the "need to calibrate" problem of the HFDF system. It is based on measuring the system response to multiple onboard near-field sources. The test is performed along with the standard calibration described in the last section, and the antenna responses to the near-field sources are stored in a reference data base. Whenever a modification is made to the topside, the near-field test is repeated and the new results are compared to the near-field reference data base. A significant difference may indicate a need to perform a full system calibration. These measurements may provide additional information beyond the "need to calibrate." For instance, they can be used to compare the effect of identical modifications on two different ships. If the near-field test results yield the same change for both ships, recalibration might need to be performed only on one ship; changes

to the calibration data for the second ship could be inferred by comparing it's near-field data with the first one's.

In order to validate the proposed approach, a simulation was performed which is briefly described as a three step procedure:

1. compute the response of the antennas due to a source placed at various locations on the ship within the near-field of the antennas,
2. perform the same set of computations after having introduced a simulated modification to the topside of the original model, and
3. compare the results to determine whether any difference is significant.

There are several near-field parameters that are varied in the simulation to determine their effect on the outcome and, perhaps, arrive at some optimum or acceptable values. They include:

1. number and location of the transmitters,
2. transmitter power level,
3. source proximity to the ship modification,
4. source proximity to antennas, and
5. type and severity of the modification.

IV. NUMERICAL MODELING AND SIMULATION OF THE CALIBRATION METHOD

A. NUMERICAL MODELING OF THE SHIP

The "need to calibrate" can be demonstrated in either of three ways:

1. full scale measurement,

2. scaled-model measurement, or

3. computer simulation.

The last, computer simulation, is the easiest because it does not require a ship (or model) and test instrumentation. Changes can be quickly simulated on the computer, whereas corresponding changes on a ship would be extremely costly. On the other hand, the numerical model does not have the fidelity of the full-scale model. However, this is not a critical problem because the "need to calibrate" procedure is only looking for relative changes in the antenna responses, not absolute values.

The ship modeling as well as the procedure simulation was performed using the code PATCH. PATCH is a frequency domain electromagnetic code based on a method-of-moments (MoM) solution to the electric field integral equation (EFIE), and can be applied to objects of arbitrary shape, both open and closed.

The code has many capabilities and they are fully described in the User's Manual [Ref. 4]. However, it is convenient to highlight the ones which were exercised during the course of the study.

PATCH uses planar triangular patches for modeling complex objects because they can easily conform to surfaces of general shape and allow variable densities over the surface of the object. The model of the DD-963 (Spruance Class Destroyer) is shown in Figure 9. The lines denote edges of flat triangular patches. The requirement for patch dimensions on smooth surfaces is that the edge lengths should typically be no longer than 1/5 to 1/10 of a wavelength. This easily satisfied at frequencies below 10MHz where the wavelength is 30m.

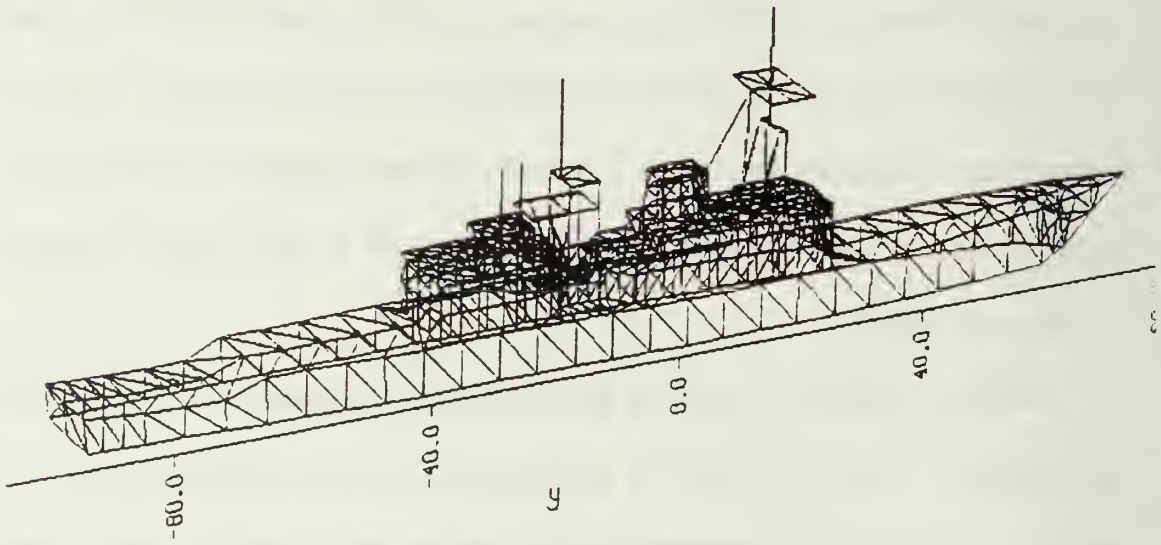

Figure 9. Patch model of the Spruance class destroyer (DD-963).

The code makes full use of the existing symmetries in the geometry of the problem by placing perfect electric or perfect magnetic conductors in place of the symmetry planes (x=0, y=0, z=0). Thus, the surface of the sea is represented by a perfect electric conductor placed at the z=0 plane.

The near-field source is a very thin tapelike structure which simulates a monopole on the ship deck. The rule of thumb for modeling thin wires is that a circular wire of radius r is equivalent to a tape width of 4r. The simulation of the near-field procedure used the following data:

1. frequency: f = 6 MHz,
2. monopole driving voltage: V=100 V,
3. monopole antenna length : λ / 10, and
4. monopole antenna width : λ / 30.

The deck-edge antennas of the HFDF system are assumed to be located along the edge of a patch as shown in Figure 10. The code provides the current

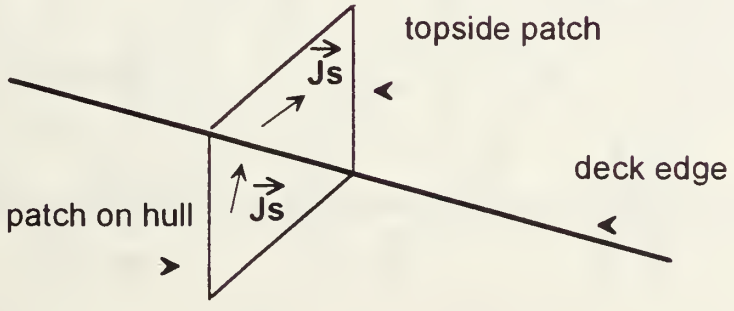

Figure 10. Antenna location on a patch edge.

densities perpendicular to each edge for all patches. The selected antenna elements are located along horizontal edges because the current crossing them is due to the vertical component of the incident electric field. The current density J_s is constant along the length of an edge. Thus, if the deck-edge antenna length is 0.5m and the edge is L, the current sensed by the loop is $I = J_s L$.

The locations considered in the simulation are:

1. Bow : Edge number 10, B-10, Figure 11.

2. Midships : Edge number 1762, M-1760, Figure 12.

3. Astern : Edge number 106, A-106, Figure 13.

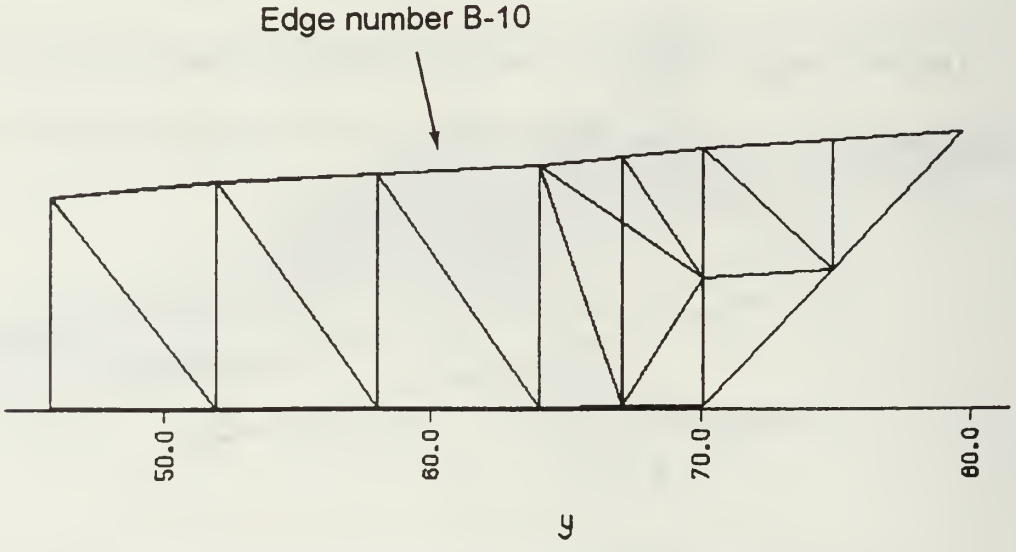

Figure 11. Antenna element on edge number 10 (bow).

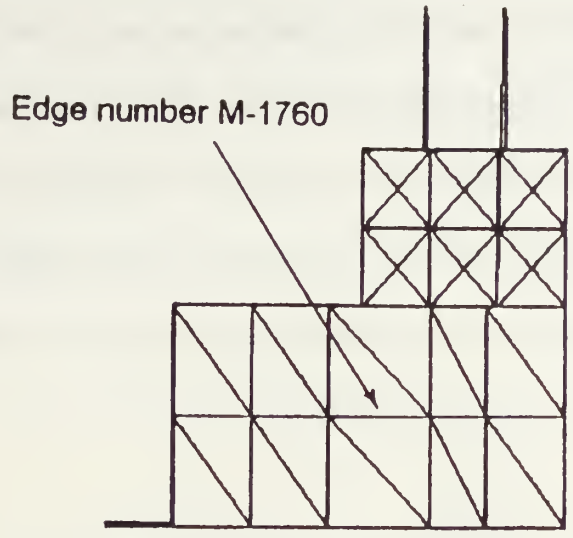

Figure 12. Antenna element on edge number 1760 (midships).

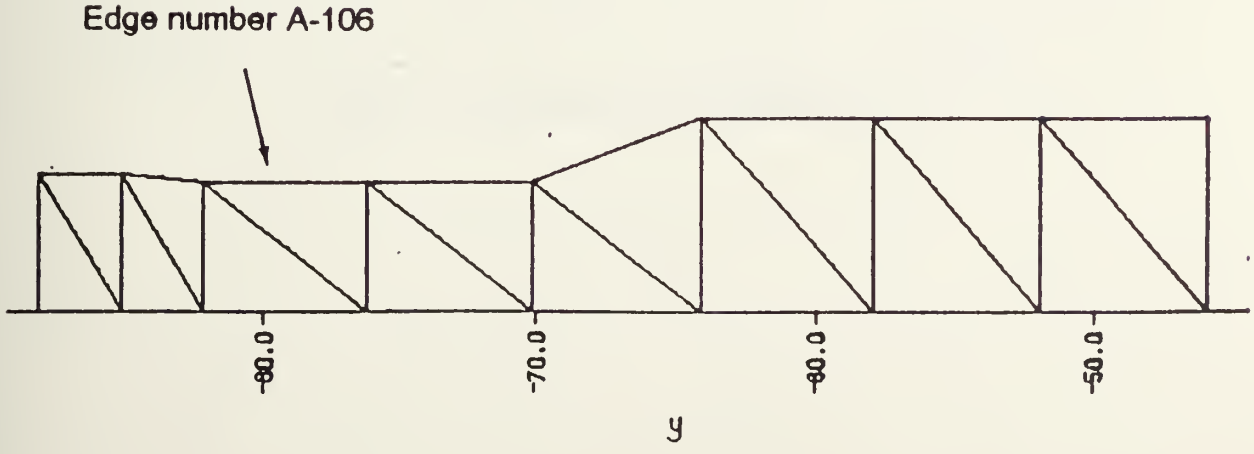

Figure 13. Antenna element on edge number 106 (astern).

B. NEAR-FIELD MEASUREMENT SIMULATION

The first step is to excite the antenna elements with a source located at various positions on the surface of the ship. PATCH is used to compute the current densities on the ship due to the source. The antenna responses are determined from the current passing across the antenna length. The coordinates of the sources considered in the simulation are shown in Figure 14. The coordinates of the strip are as shown in Table 1:

TABLE 1. STRIP COORDINATES.

LOCATION	x_1 , x_4	x_2 , x_3	y	z_1 , z_4	z_2 , z_3
A	-1	1	75	10.5	16.5
B	-1	1	40	8	14
C	-1	1	-60	8	14
D	-1	1	-90	6	12

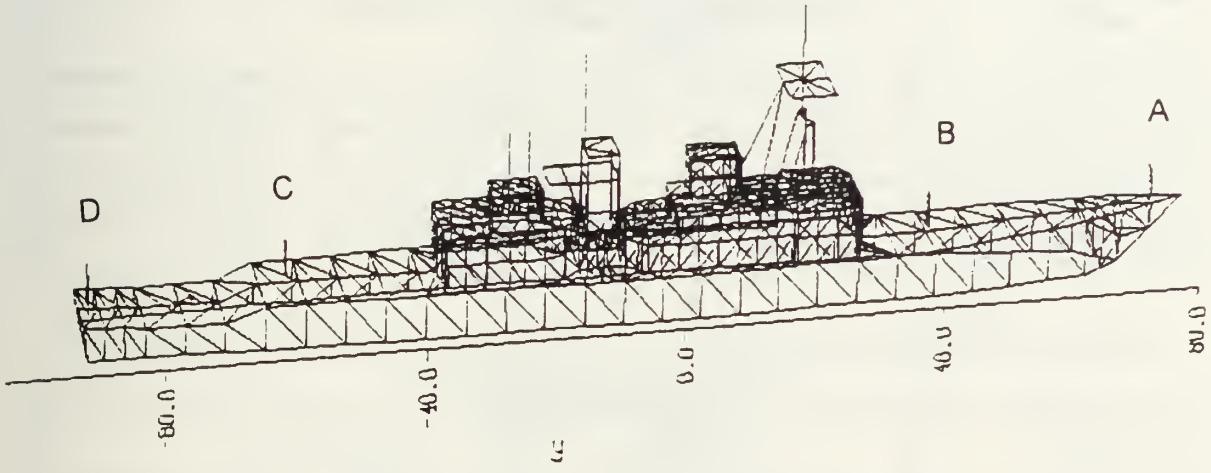

Figure 14. Near-field source locations.

The construction and excitation of the monopole is illustrated in Figure 15. Several radiation patterns for the monopole are presented in Appendix A. Computed current data is given in Tables 2, 3, 4, and 5 for transmit locations A, B, C, and D respectively.

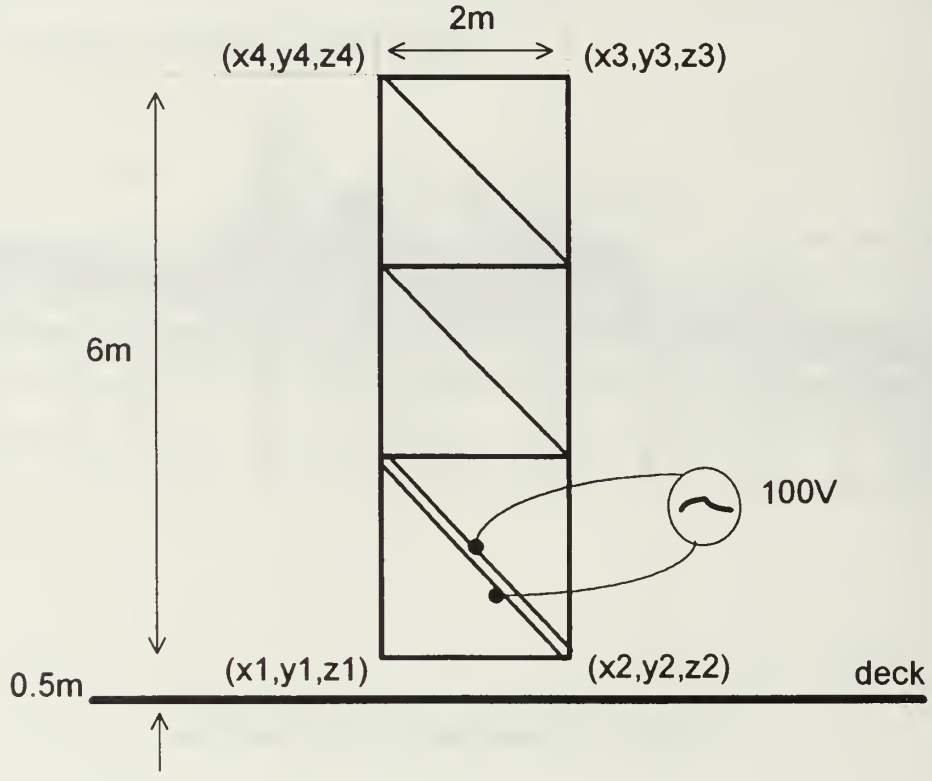

Figure 15. Transmit monopole and its excitation.

TABLE 2. COMPUTED DATA FOR THE ORIGINAL SHIP CONFIGURATION. TRANSMIT LOCATION A.

	Current Density J (A/m)		Current I (A)
Edge	**Magnitude**	**Phase**	**I = 0.5 x | J |**
B-10	0.81876×10^{-3}	-71.654	0.40938×10^{-2}
M-1760	0.98694×10^{-4}	-96.254	0.49347×10^{-4}
A-106	0.11971×10^{-4}	-39.001	0.05985×10^{-4}

TABLE 3. COMPUTED DATA FOR THE ORIGINAL SHIP CONFIGURATION. TRANSMIT LOCATION B.

	Current Density J (A/m)		Current I (A)
Edge	**Magnitude**	**Phase**	**I = 0.5 x | J |**
B-10	0.19715×10^{-3}	29.841	0.098575×10^{-3}
M-1760	0.52686×10^{-4}	144.322	0.26343×10^{-4}
A-106	0.58949×10^{-5}	-121.743	0.294745×10^{-5}

TABLE 4. COMPUTED DATA FOR THE ORIGINAL SHIP CONFIGURATION. TRANSMIT LOCATION C.

	Current Density J (A/m)		Current I (A)
Edge	**Magnitude**	**Phase**	**I = 0.5 x | J |**
B-10	0.22133×10^{-4}	-2.144	0.110665×10^{-4}
M-1760	0.72595×10^{-3}	-101.293	0.362975×10^{-3}
A-106	0.20377×10^{-3}	-59.492	0.101885×10^{-3}

TABLE 5. COMPUTED DATA FOR THE ORIGINAL SHIP CONFIGURATION. TRANSMIT LOCATION D.

	Current Density J (A/m)		Current I (A)
Edge	**Magnitude**	**Phase**	**I = 0.5 x | J |**
B-10	0.23681×10^{-4}	167.264	0.118405×10^{-4}
M-1760	0.59780×10^{-3}	63.377	0.2989×10^{-3}
A-106	0.93215×10^{-3}	42.371	0.466075×10^{-3}

Next, modification of the ship is simulated by adding a cylinder (possibly representing a gun) at either the bow or the stern (see Figures 16 through 18). The cylinder was constructed with height of 3m and radius of 1m. The current calculations described above are repeated for the same locations. The results are summarized in Tables 6, 7, 8, and 9 for the forward modification, and Tables 10, 11, 12, and 13 for the aft modification.

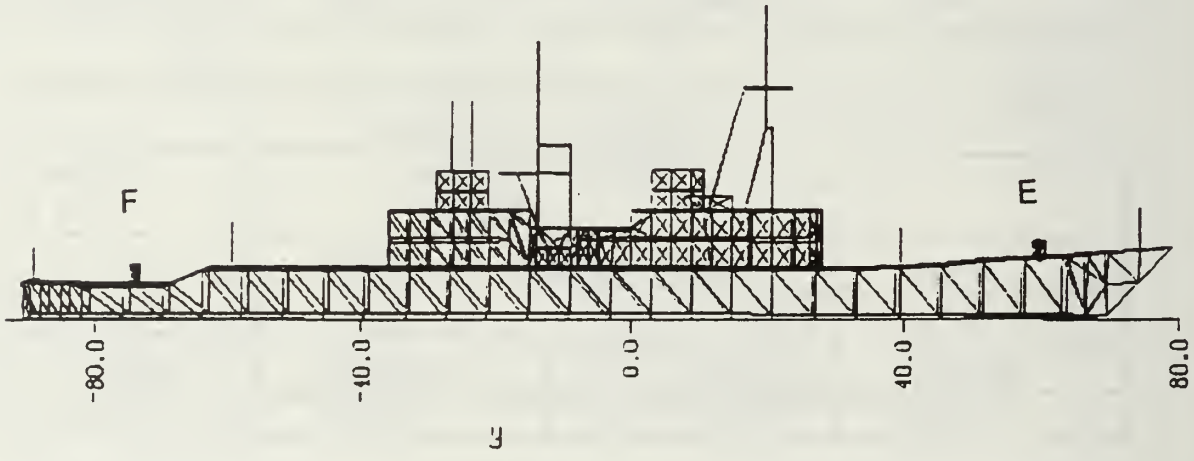

Figure 16. Simulated modifications on the topside of the ship (E and F).

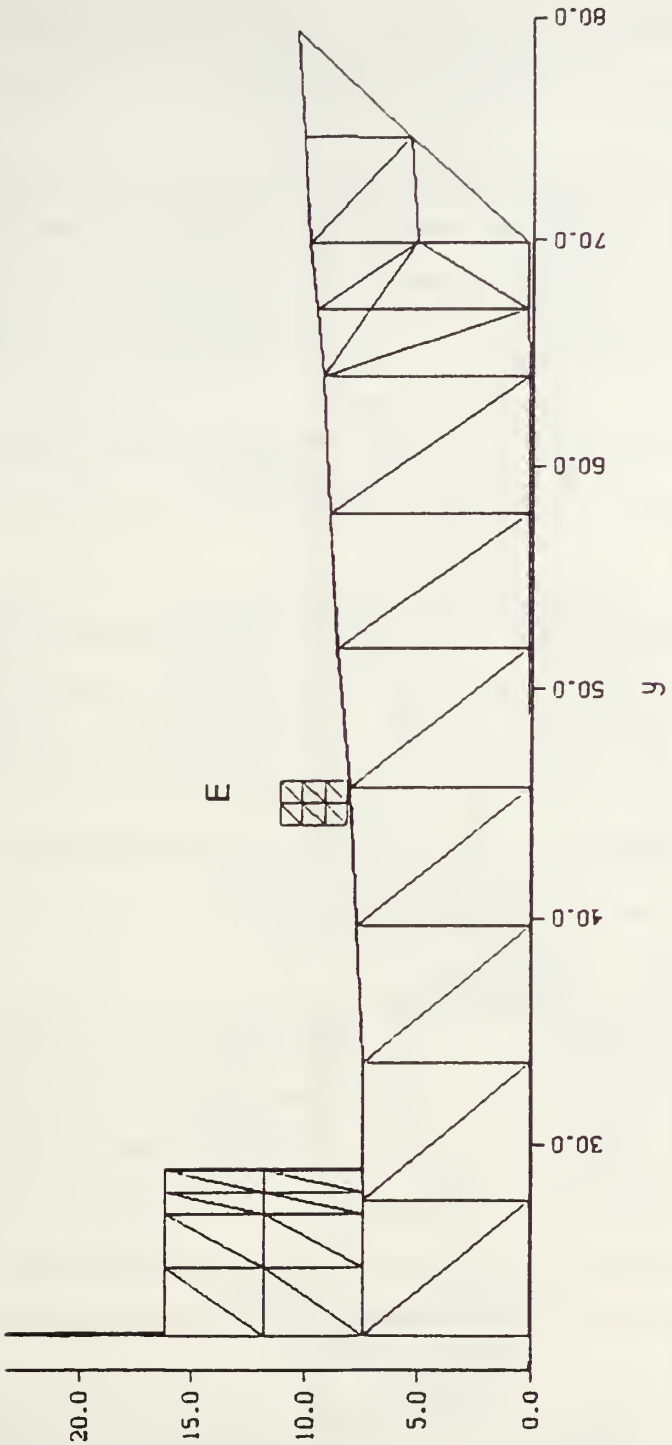

Figure 17. Enlarged view of the modification at the bow.

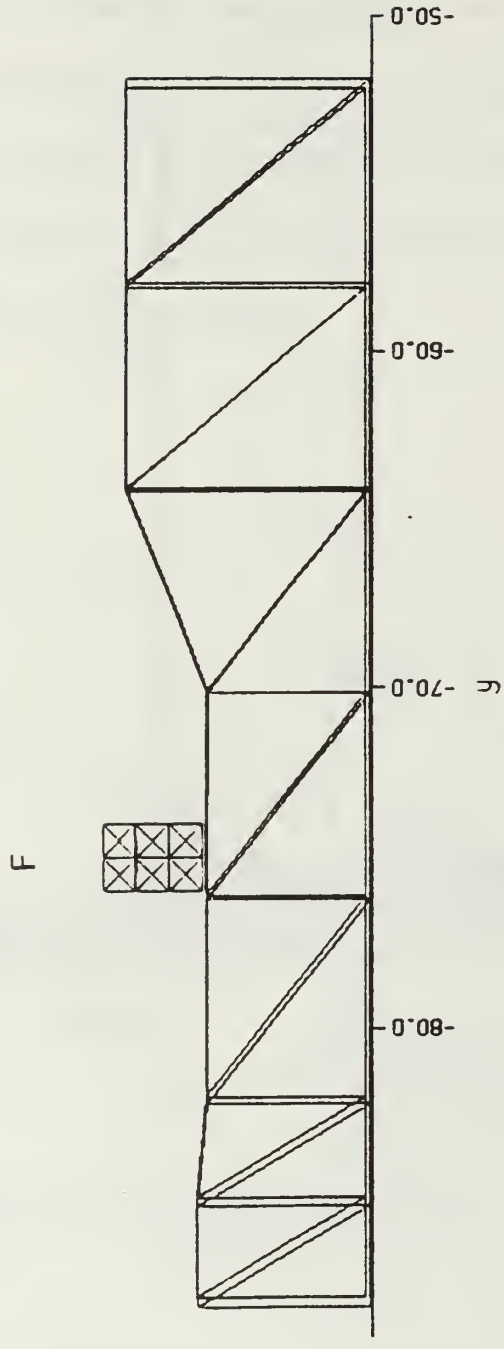

Figure 18. Enlarged view of the modification at the stern.

TABLE 6. COMPUTED DATA FOR THE MODIFIED (BOW) CONFIGURATION.
TRANSMIT LOCATION A .

	Current Density J (A/m)		Current I (A)
Edge	**Magnitude**	**Phase**	**I = 0.5 x | J |**
B-10	0.83021×10^{-3}	-73.414	0.41510×10^{-3}
M-1760	0.99373×10^{-4}	-96.343	0.49686×10^{-4}
A-106	0.12049×10^{-4}	-39.060	0.06024×10^{-4}

TABLE 7. COMPUTED DATA FOR THE MODIFIED (BOW) CONFIGURATION.
TRANSMIT LOCATION B .

	Current Density J (A/m)		Current I (A)
Edge	**Magnitude**	**Phase**	**I = 0.5 x | J |**
B-10	0.19689×10^{-3}	29.080	0.098445×10^{-3}
M-1760	0.55421×10^{-4}	146.557	0.277105×10^{-4}
A-106	0.58293×10^{-5}	-122.617	0.291465×10^{-5}

TABLE 8. COMPUTED DATA FOR THE MODIFIED (BOW) CONFIGURATION.
TRANSMIT LOCATION C.

	Current Density J (A/m)		Current I (A)
Edge	**Magnitude**	**Phase**	**I = 0.5 x | J |**
B-10	0.22026×10^{-4}	-2.532	0.11013×10^{-4}
M-1760	0.72598×10^{-3}	-101.289	0.36299×10^{-3}
A-106	0.20377×10^{-3}	-59.489	0.101885×10^{-3}

TABLE 9. COMPUTED DATA FOR THE MODIFIED (BOW) CONFIGURATION.
TRANSMIT LOCATION D.

	Current Density J (A/m)		Current I (A)
Edge	**Magnitude**	**Phase**	**I = 0.5 x | J |**
B-10	0.23560×10^{-4}	166.910	0.1178×10^{-4}
M-1760	0.59751×10^{-3}	64.448	0.298755×10^{-3}
A-106	0.93214×10^{-3}	42.371	0.46607×10^{-3}

TABLE 10. COMPUTED DATA FOR THE MODIFIED (AFT) CONFIGURATION. TRANSMIT LOCATION A.

	Current Density J (A/m)		Current I (A)
Edge	**Magnitude**	**Phase**	I = 0.5 x | J |
B-10	0.10592×10^{-2}	-67.518	0.05296×10^{-2}
M-1760	0.13008×10^{-3}	-95.200	0.06504×10^{-3}
A-106	0.15443×10^{-4}	-33.833	0.077215×10^{-4}

TABLE 11. COMPUTED DATA FOR THE MODIFIED (AFT) CONFIGURATION. TRANSMIT LOCATION B.

	Current Density J (A/m)		Current I (A)
Edge	**Magnitude**	**Phase**	**I = 0.5 x | J |**
B-10	0.13313×10^{-3}	22.939	0.066565×10^{-3}
M-1760	0.40565×10^{-4}	144.390	0.202825×10^{-4}
A-106	0.42751×10^{-5}	-125.496	0.213755×10^{-5}

TABLE 12. COMPUTED DATA FOR THE MODIFIED (AFT) CONFIGURATION. TRANSMIT LOCATION C.

	Current Density J (A/m)		Current I (A)
Edge	**Magnitude**	**Phase**	**I = 0.5 x | J |**
B-10	0.17552×10^{-4}	-2.643	0.08776×10^{-4}
M-1760	0.57529×10^{-3}	-101.908	0.287645×10^{-3}
A-106	0.19817×10^{-3}	-65.225	0.099085×10^{-3}

TABLE 13. COMPUTED DATA FOR THE MODIFIED (AFT) CONFIGURATION. TRANSMIT LOCATION D.

	Current Density J (A/m)		Current I (A)
Edge	**Magnitude**	**Phase**	**I = 0.5 x | J |**
B-10	0.23742×10^{-4}	167.151	0.11871×10^{-4}
M-1760	0.59929×10^{-3}	64.315	0.299645×10^{-3}
A-106	0.92695×10^{-3}	42.358	0.463475×10^{-3}

The difference in the values of the current that were observed can be quantized in terms of their fractional change which is defined as follows:

$$FRACTIONAL\ CHANGE = \frac{|I_{modified} - I_{original}|}{I_{original}} \times 100. \qquad (3)$$

The calculations for the fractional changes were performed only for the cases of the deck-edge antennas at the extremes of the ship, because these are representative of the largest and smallest antenna-source distances. The results are summarized in Table 14.

TABLE 14. FRACTIONAL CHANGES IN THE DECK-EDGE ANTENNA CURRENTS.

DECK-EDGE ANTENNA LOCATION	SOURCE LOCATION	MODIFICATION	FRACTIONAL CHANGE
B-10	A	BOW	1.39%
B-10	B	BOW	0.13%
B-10	C	BOW	0.48%
B-10	D	BOW	0.51%
A-106	A	ASTERN	2.9%
A-106	B	ASTERN	2.7%
A-106	C	ASTERN	2.74%
A-106	D	ASTERN	0.55%

The excitation of 100V was chosen to give approximately the same order of magnitude power density at the nearest deck-edge antenna. For the current at-sea calibration, the transmit site uses a log-periodic dipole ($G \approx 2dBi$) and a CW power of P_t=500W. The field strength at the ship, with the ship being at a distance of R=10nm from the transmitting site (Figure 8), is

$$|E| = \frac{\sqrt{30 P_t G_t}}{R} = 0.00832 V/m \qquad (4)$$

and therefore, the power density at the ship is

$$P_d = \frac{P_t G_t}{4\pi R^2} = 1.84 x 10^{-7} W/m^2. \qquad (5)$$

For comparison, the power densities at the stern deck-edge antenna (edge number A-106) were computed for the near-field excitations A and D. The data is shown in Table 15 at the coordinates x=7.2 , y=-84 , z=4.8. Both bow and stern excitations with the sources residing at the far ends of the original ship (locations A and D) were considered.

TABLE 15. COMPUTED ELECTRIC AND MAGNETIC FIELD COMPONENTS.

SOURCE LOCATION	ELECTRIC and MAGNETIC FIELD COMPONENTS	MAGNITUDE of ELECTRIC and MAGNETIC FIELD COMPONENTS
A	$Ex=0.64648x10^{-1}-j0.15699x10^{-2}$	$\|Ex\|=0.0647$
	$Ey=0.52109x10^{-2}-j0.68087x10^{-3}$	$\|Ey\|=0.0053$
	$Ez=-0.33703x10^{-1}+j0.26763x10^{-2}$	$\|Ez\|=0.0038$
	$Hx=0.744887x10^{-4}+j0.23441x10^{-4}$	$\|Hx\|=7.8x10^{-5}$
	$Hy=-0.42164x10^{-5}-j0.20512x10^{-4}$	$\|Hy\|=2.09x10^{-5}$
	$Hz=-0.12120x10^{-3}-j0.62355x10^{-4}$	$\|Hz\|=1.36x10^{-4}$
D	$Ex=-0.16615-j0.56306$	$\|Ex\|=0.5871$
	$Ey=0.15930x10^{-1}-j0.46265x10^{-3}$	$\|Ey\|=0.0159$
	$Ez=-0.85361x10^{-1}-j0.27030$	$\|Ez\|=0.2835$
	$Hx=-0.26022x10^{-3}-j0.47239x10^{-3}$	$\|Hx\|=5.4x10^{-4}$
	$Hy=0.71199x10^{-3}+j0.67410x10^{-3}$	$\|Hy\|=9.8x10^{-4}$
	$Hz=0.55981x10^{-3}+j0.10948x10^{-2}$	$\|Hz\|=0.0012$

The average power density can be calculated using the formula: $P_{av}=|\mathbf{E}|^2/\eta$, where η is the free-space impedance ($\eta=377\Omega$). The power densities due to the vertical component of the **E**-field ($\mathbf{E}_z$) and the total **E**-field are shown in Table 16.

TABLE 16. COMPUTED POWER DENSITIES.

SOURCE LOCATION	$\lvert E_z\rvert^2/\eta$	$\lvert E\rvert^2/\eta$
A	3.83023×10^{-8} W/m^2	3.47×10^{-6} W/m^2
D	2.13188×10^{-4} W/m^2	3.04×10^{-3} W/m^2

These densities are roughly comparable to the power densities in the far-field test method given by (5), at least at location D.

C. PLANE WAVE SIMULATION

The second part of this simulation examines the response of the antenna elements due to an incident plane wave. This provides an estimate of the fractional change in current typical of the at-sea calibration method. Wave angles considered range from the bow for $\theta_i=90^0$ and $\phi_i=90^0$, to broadside for $\theta_i=90^0$ and $\phi_i=0^0$. The measurements were made at the same edges as previously noted for both the original and the modified model, and are shown in the following Tables 17 through 25.

TABLE 17. COMPUTATION DATA FOR THE ORIGINAL CONFIGURATION. PLANE WAVE EXCITATION ($\theta_i = 90^0$, $\phi_i = 0^0$).

	Current Density J (A/m)		Current I (A)
Edge	**Magnitude**	**Phase**	**I = 0.5 x | J |**
B-10	0.82586×10^{-2}	-151.39	0.41293×10^{-2}
M-1760	0.97366×10^{-2}	54.111	0.48683×10^{-2}
A-106	0.84297×10^{-2}	-122.784	0.42148×10^{-2}

TABLE 18. COMPUTATION DATA FOR THE ORIGINAL CONFIGURATION. PLANE WAVE EXCITATION ($\theta_i = 90^0$, $\phi_i = 45^0$).

	Current Density J (A/m)		Current I (A)
Edge	**Magnitude**	**Phase**	**I=0.5x| J |**
B-10	0.77574×10^{-2}	-151.43	0.38787×10^{-2}
M-1760	0.38094×10^{-2}	-88.6	0.19047×10^{-2}
A-106	0.53185×10^{-2}	-162.08	0.26592×10^{-2}

TABLE 19. COMPUTATION DATA FOR THE ORIGINAL CONFIGURATION. PLANE WAVE EXCITATION ($\theta_i = 90^0$, $\phi_i = 90^0$).

	Current Density J (A/m)		Current I (A)
Edge	**Magnitude**	**Phase**	**I=0.5x|J|**
B-10	0.45823×10^{-2}	-106.090	$0.22.911 \times 10^{-2}$
M-1760	0.18364×10^{-2}	-43.143	0.09182×10^{-2}
A-106	0.74648×10^{-3}	-23.478	0.37324×10^{-3}

TABLE 20. COMPUTED DATA FOR THE MODIFIED (BOW) CONFIGURATION. PLANE WAVE EXCITATION ($\theta_i = 90^0$, $\phi_i = 0^0$).

	Current Density J (A/m)		Current I (A)
Edge	**Magnitude**	**Phase**	**I = 0.5 x | J |**
B-10	0.83451×10^{-2}	-151.03	0.41725×10^{-2}
M-1760	0.97341×10^{-2}	54.117	0.48670×10^{-2}
A-106	0.84300×10^{-2}	-122.783	0.4215×10^{-2}

TABLE 21. COMPUTED DATA FOR THE MODIFIED (BOW) CONFIGURATION. PLANE WAVE EXCITATION ($\theta_i = 90^0$, $\phi_i = 45^0$).

	Current Density J (A/m)		Current I (A)
Edge	**Magnitude**	**Phase**	**I = 0.5 x | J |**
B-10	0.77314×10^{-2}	-151.34	0.38657×10^{-2}
M-1760	0.38088×10^{-2}	-88.59	0.19044×10^{-2}
A-106	0.53185×10^{-2}	-162.08	0.265925×10^{-2}

TABLE 22. COMPUTED DATA FOR THE MODIFIED (BOW) CONFIGURATION. PLANE WAVE EXCITATION ($\theta_i = 90^0$, $\phi_i = 90^0$).

	Current Density J (A/m)		Current I (A/m)
Edge	**Magnitude**	**Phase**	**I = 0.5 x | J |**
B-10	0.47561×10^{-2}	-107.37	0.23780×10^{-2}
M-1760	0.18269×10^{-2}	-43.5	0.09134×10^{-2}
A-106	0.74647×10^{-3}	-23.62	0.37323×10^{-3}

TABLE 23. COMPUTED DATA FOR THE MODIFIED (AFT) CONFIGURATION. PLANE WAVE EXCITATION ($\theta_i = 90^0$, $\phi_i = 0^0$).

	Current Density J (A/m)		Current I (A)
Edge	**Magnitude**	**Phase**	**I = 0.5 x | J |**
B-10	0.82579×10^{-2}	-151.39	0.41289×10^{-2}
M-1760	0.97384×10^{-2}	53.97	0.48692×10^{-2}
A-106	0.84502×10^{-2}	-122.92	0.42251×10^{-2}

TABLE 24. COMPUTED DATA FOR THE MODIFIED (AFT) CONFIGURATION. PLANE WAVE EXCITATION ($\theta_i = 90^0$, $\phi_i = 45^0$).

	Current Density J (A/m)		Current I (A)
Edge	**Magnitude**	**Phase**	**I = 0.5 x | J |**
B-10	0.77576×10^{-2}	151.423	0.38788×10^{-2}
M-1760	0.38185×10^{-2}	-88.395	0.19092×10^{-2}
A-106	0.53296×10^{-2}	162.172	0.26648×10^{-2}

TABLE 25. COMPUTED DATA FOR THE MODIFIED (AFT) CONFIGURATION. PLANE WAVE EXCITATION ($\theta_i = 90^0$, $\phi_i = 90^0$).

	Current Density J (A/m)		Current I (A)
Edge	**Magnitude**	**Phase**	**I = 0.5 x | J |**
B-10	0.45830×10^{-2}	-106.09	0.22915×10^{-2}
M-1760	0.18182×10^{-2}	-43.09	0.09091×10^{-2}
A-106	0.75617×10^{-3}	-22.87	0.37808×10^{-2}

In order to quantify the severity of the modifications, the fractional changes are calculated as in the previous section. Similarly, as in the previous section, the calculations were performed only for the deck-edge antennas at the extreme front and back of the ship; that is, for the antennas residing on edges B-10 and A-106. The results of these calculations are listed in Table 26.

TABLE 26. FRACTIONAL CHANGES IN THE DECK-EDGE ANTENNA CURRENTS.

DECK-EDGE ANTENNA LOCATION	PLANE WAVE DIRECTION OF INCIDENCE	MODIFICATION	FRACTIONAL CHANGE
B-10	$\theta_i = 90^0$ $\phi_i = 0^0$	BOW	1.05%
B-10	$\theta_i = 90^0$ $\phi_i = 0^0$	ASTERN	0.0035%
B-10	$\theta_i = 90^0$ $\phi_i = 45^0$	BOW	0.33%
B-10	$\theta_i = 90^0$ $\phi_i = 45^0$	ASTERN	0.0025%
B-10	$\theta_i = 90^0$ $\phi_i = 90^0$	BOW	3.79%
B-10	$\theta_i = 90^0$ $\phi_i = 90^0$	ASTERN	1.29%
A-106	$\theta_i = 90^0$ $\phi_i = 0^0$	BOW	0.0035%
A-106	$\theta_i = 90^0$ $\phi_i = 0^0$	ASTERN	0.24%
A-106	$\theta_i = 90^0$ $\phi_i = 45^0$	BOW	0%
A-106	$\theta_i = 90^0$ $\phi_i = 45^0$	ASTERN	0.20%
A-106	$\theta_i = 90^0$ $\phi_i = 90^0$	BOW	0.0013%
A-106	$\theta_i = 90^0$ $\phi_i = 90^0$	ASTERN	1.29%

V. CONCLUSIONS

In this study, an investigation of a new approach in dealing with the "need to calibrate" problem of shipboard HFDF antennas was conducted. This approach is based on measuring the system response to multiple on-board near-field sources. The test is performed along with the standard calibration, and the antenna responses to the near-field sources are stored in a reference database. Whenever a modification is made to the topside, the near-field test is repeated and the new results are compared to the reference database. A significant difference may indicate a need to perform a full system calibration.

In order to validate the proposed approach, a simulation was performed, which can be described as a three step procedure:

1. compute the response of the antennas due to a source placed at various locations on the ship within the near-field of the antennas,
2. perform the same set of computations after having introduced a simulated modification to the topside of the original model, and
3. compare the results to determine whether any difference is significant.

The simulation results were characterized by the fractional change in current across selected edges before and after modifications. To provide a reference, the at-sea calibration was also simulated and the fractional changes found

to be comparable to the near-field case. In fact, the fractional change tended to be larger for the near-field excitation than the plane wave excitation.

An attempt was made to keep the power densities approximately equal for the plane wave and near-field excitations. In spite of this, the current densities induced on the ship differed by approximately an order of magnitude (higher in the plane wave case).

Based on the results of the few calculations performed in this study, it appears that the near-field method is more sensitive to topside changes than the at-sea method. This has both advantages and disadvantages. The advantage is that if no fractional change is observed for a topside modification, then one can be confident that the calibration voltages are still valid. On the other hand, small fractional changes in the near-field case can probably be disregarded. However, it is crucial that a fractional change "threshold" be established.

In an effort to set a calibration threshold based on fractional changes in the near-field, further comparisons should be made between the near-field and the plane wave excitations. Furthermore, both significant and insignificant modifications should be examined. A significant modification is one that is known to cause the reference voltages to become invalid; an insignificant modification does not invalidate the calibration. Other areas that should be investigated are convergance of the PATCH model and calculation of the CIDF coefficients for near-field sources.

APPENDIX

The radiation patterns of the monopole at various locations are given in this Appendix. These patterns were computed in the $\phi=90^0$ plane and for the original ship configuration only, since the modifications were shown to have no significant impact on the patterns. The patterns for the different source locations are shown in Figures A1 to A8.

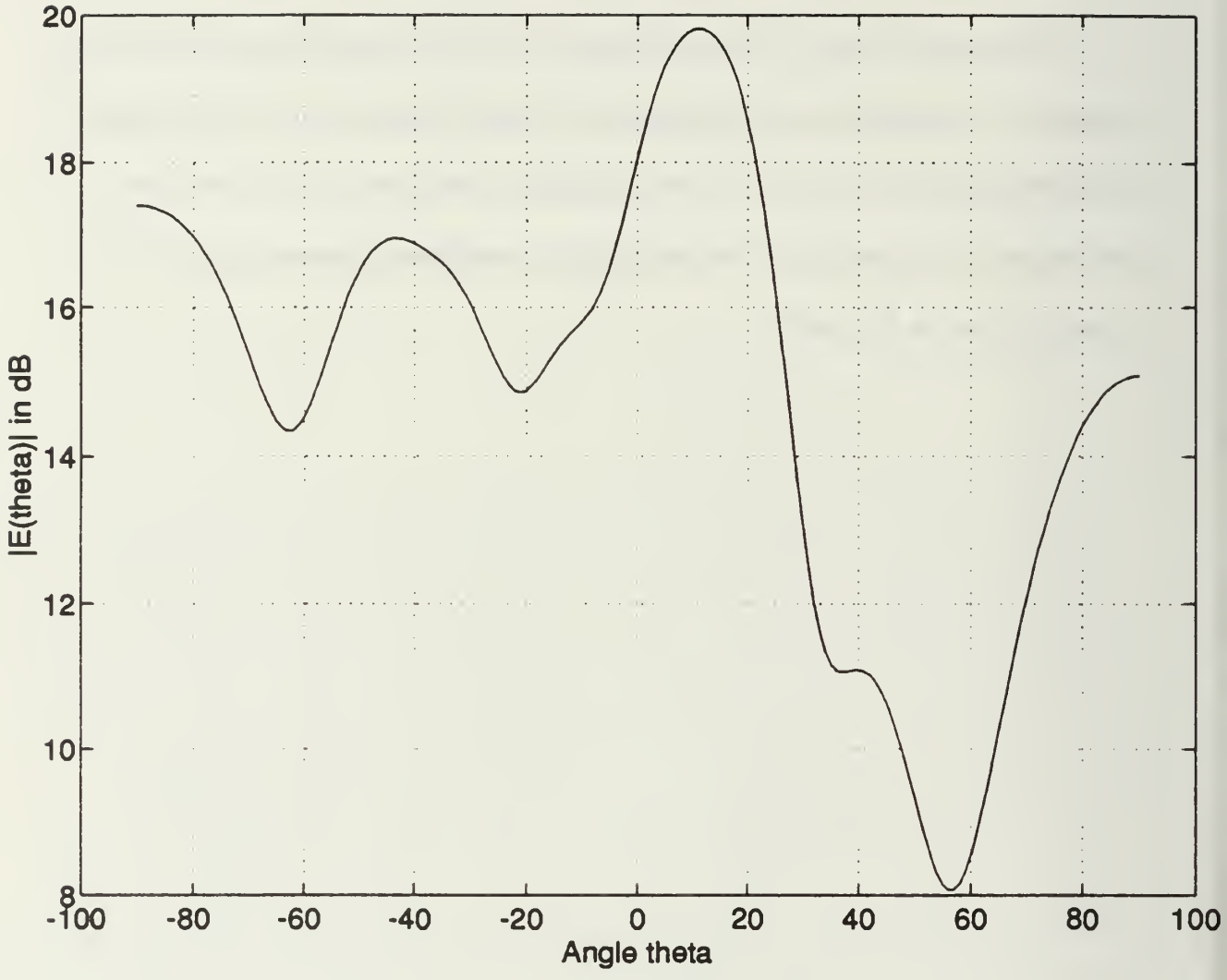

Figure A1. Original ship. E(θ) pattern for the case of excitation at the bow (location A).

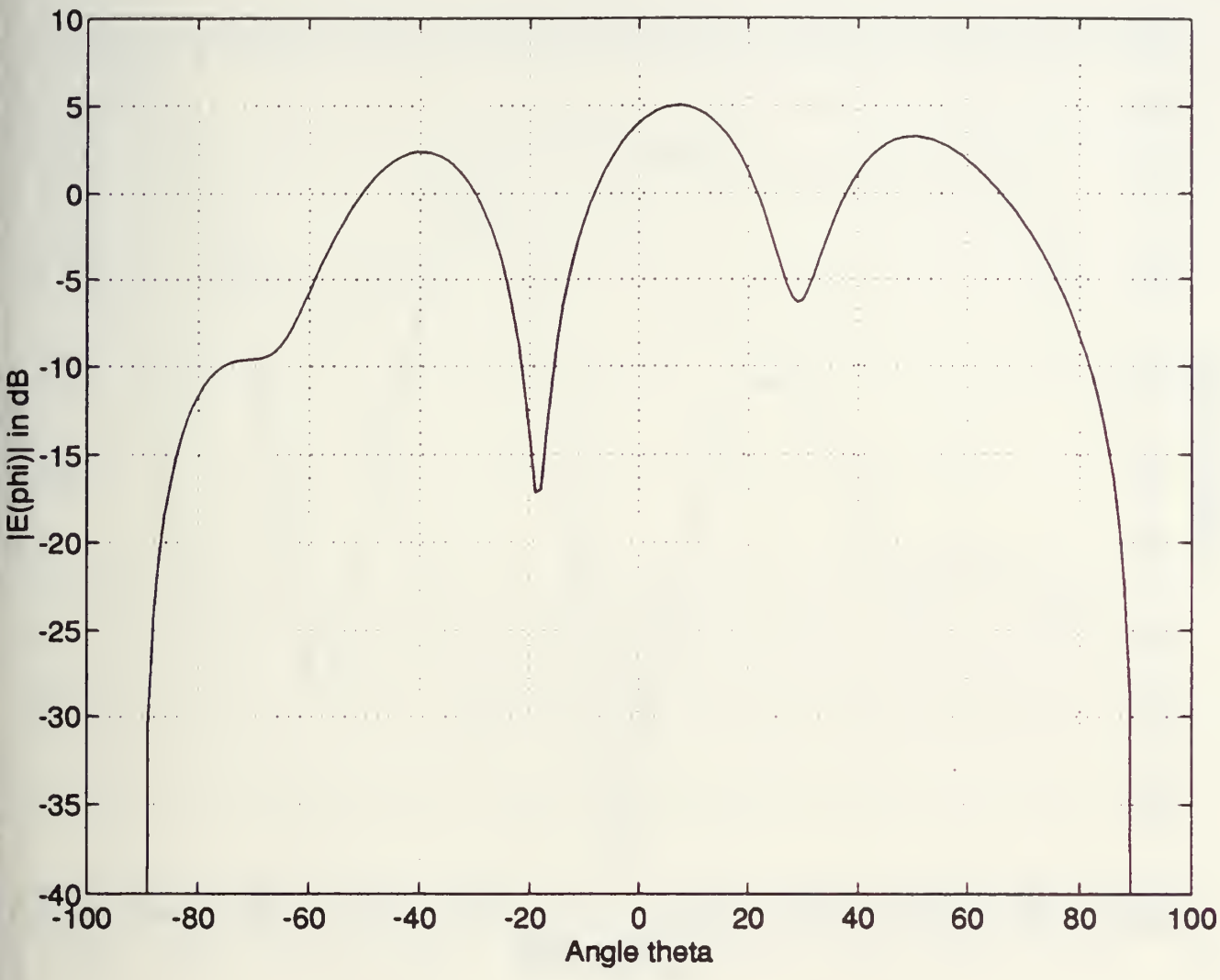

Figure A2. Original ship. E(ϕ) pattern for the case of excitation at the bow (location A).

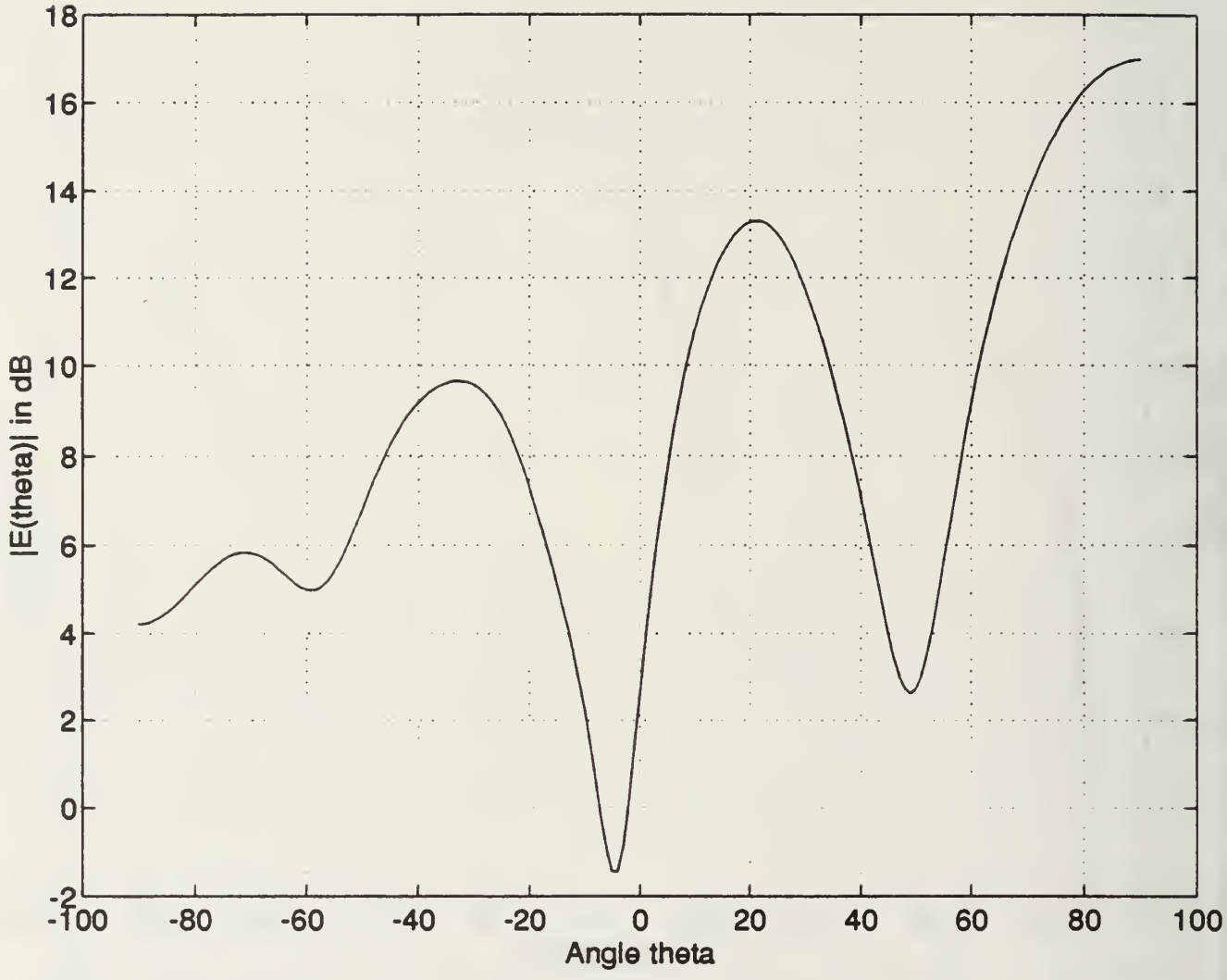

Figure A3. Original ship. E(θ) pattern for the case of excitation at the bow (location B).

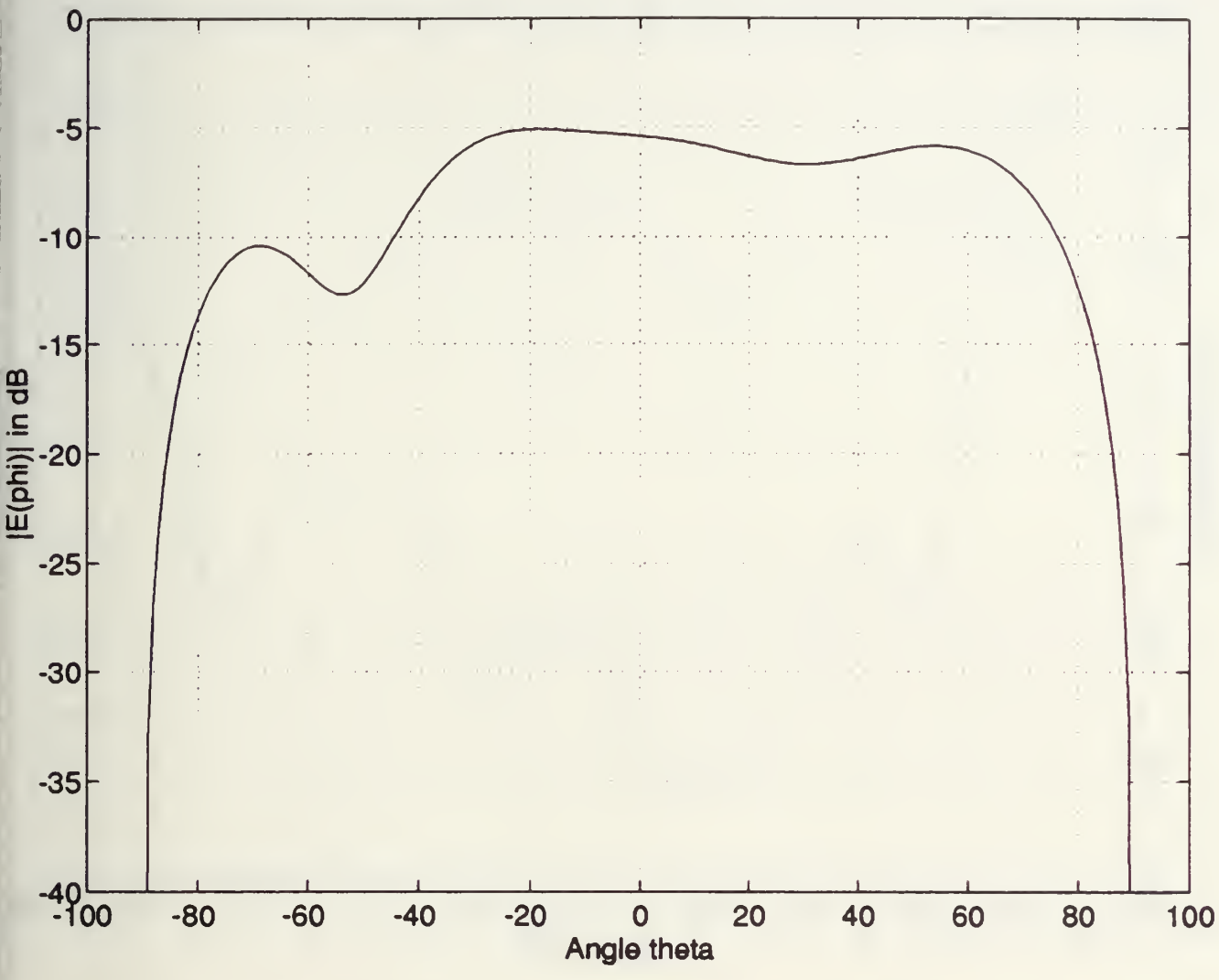

Figure A4. Original ship. E(ϕ) pattern for the case of excitation at the bow (location B).

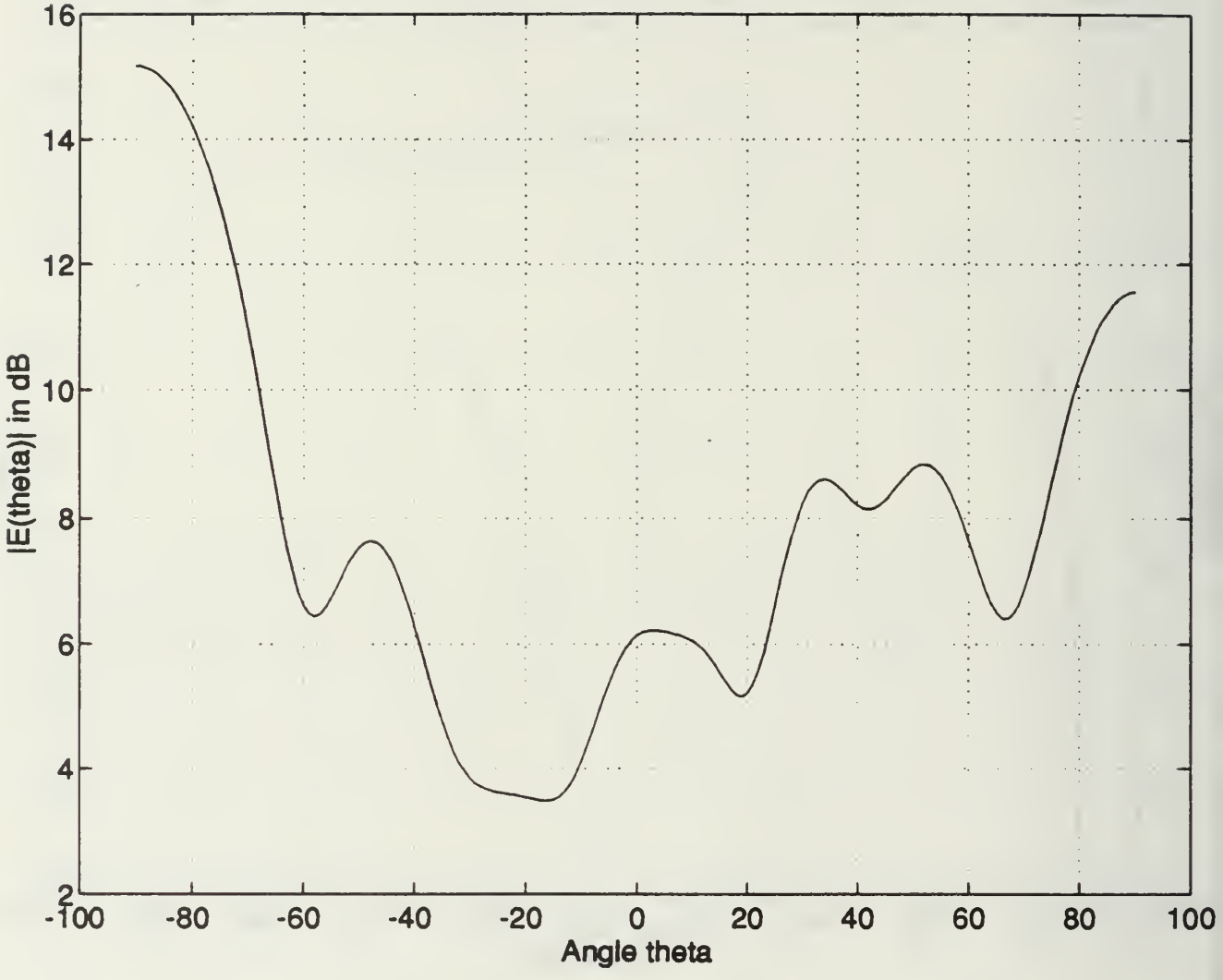

Figure A5. Original ship. E(θ) pattern for the case of excitation at the stern (location C).

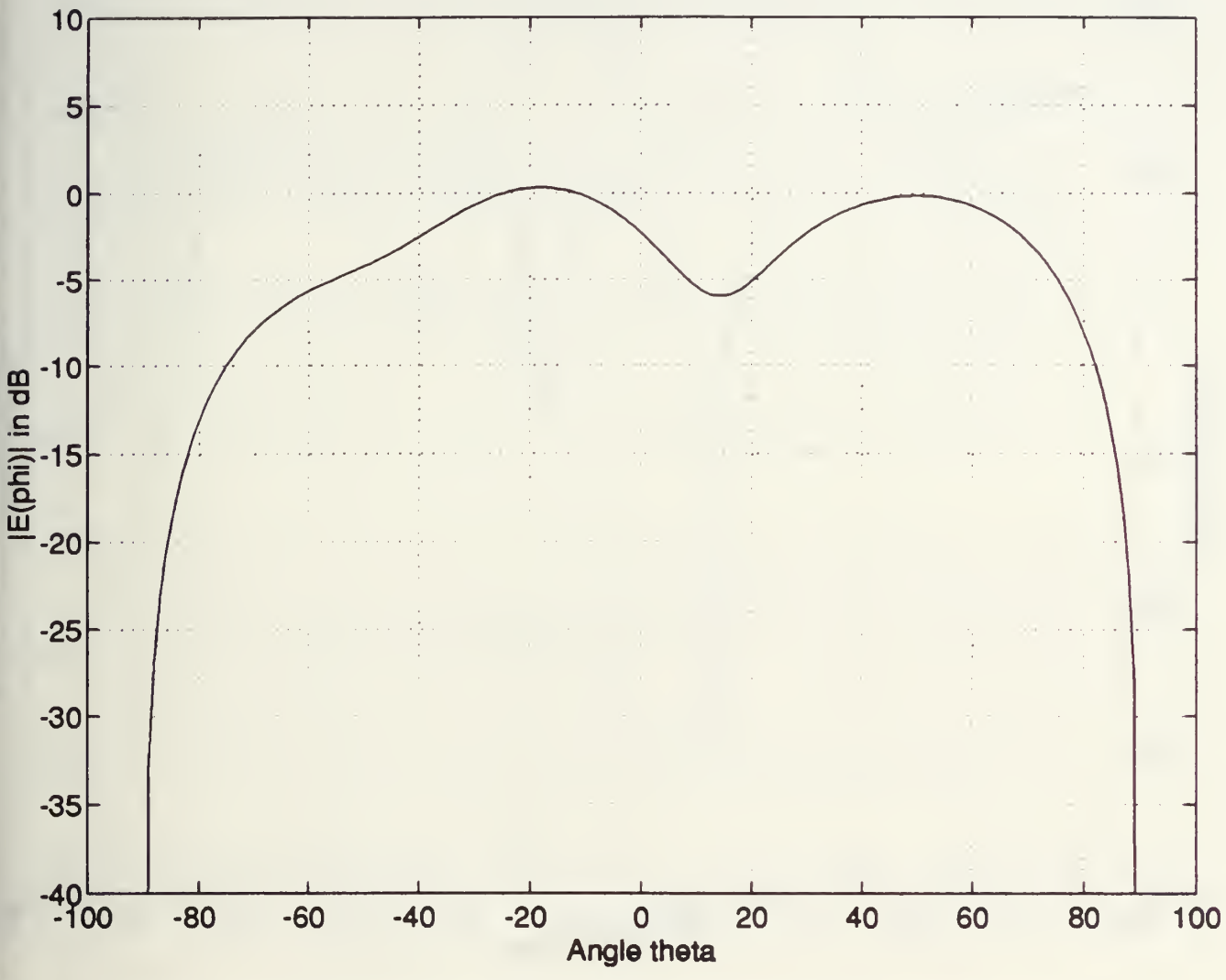

Figure A6. Original ship. E(ϕ) pattern for the case of excitation at the stern (location C).

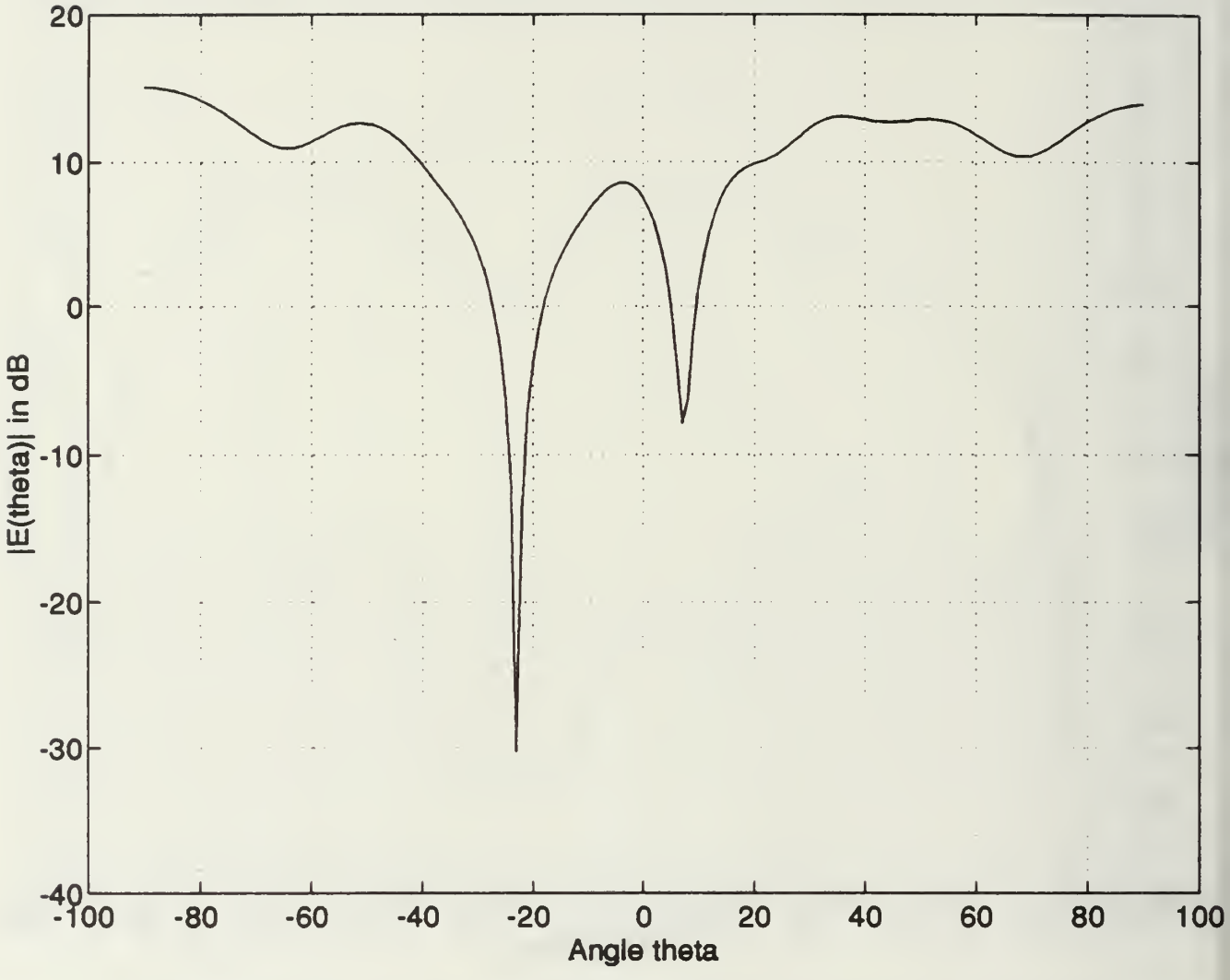

Figure A7. Original ship. E(θ) pattern for the case of excitation at the stern (location D).

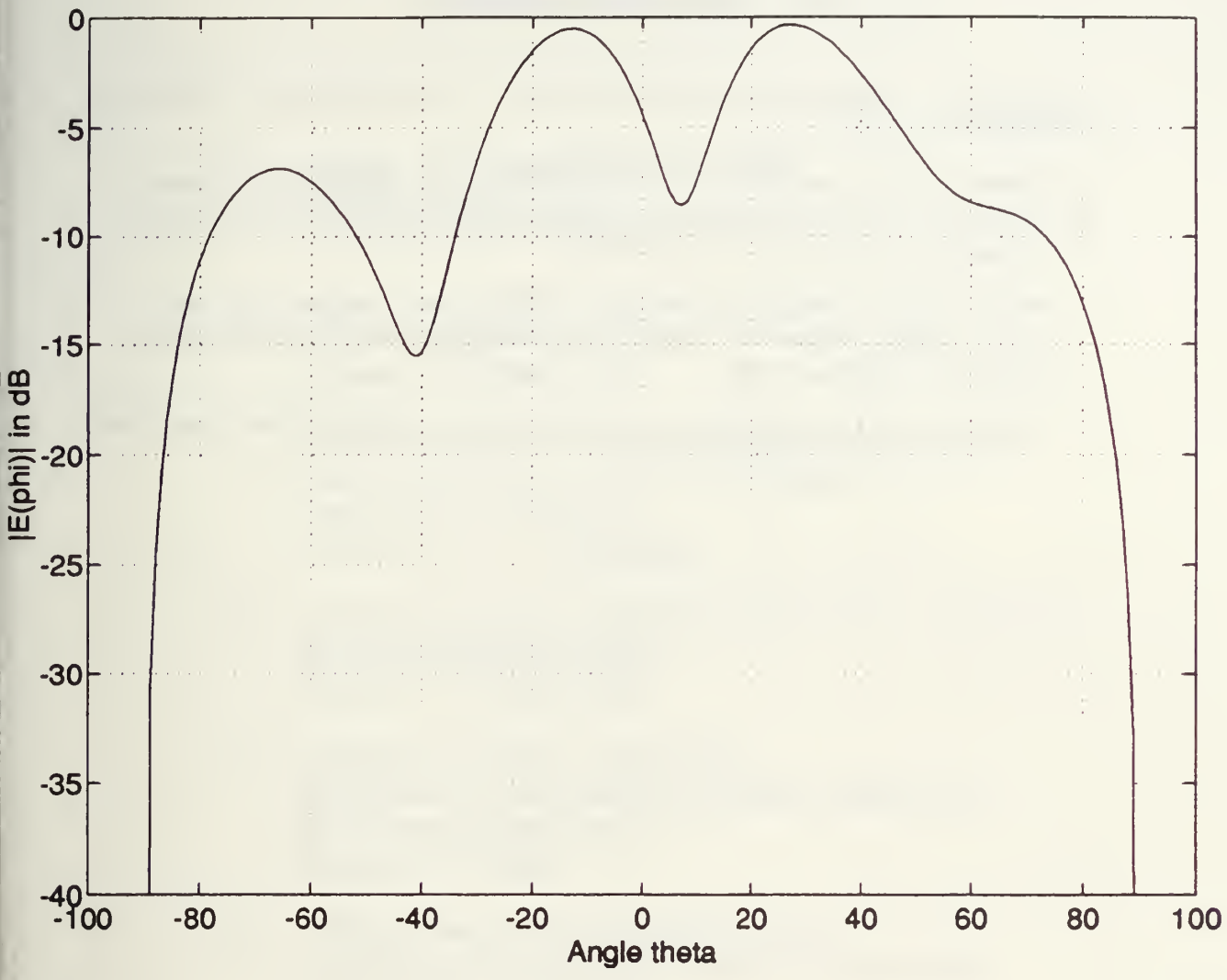

Figure A8. Original ship. E(ϕ) pattern for the case of excitation at the stern (location D).

LIST OF REFERENCES

1. Paul, C.R., *Introduction to Electromagnetic Compatibility*, John Wiley and Sons, Inc., 1992.
2. Pettengill, R.C., Garland, H.T., and Meindl, J.D., "Receiving Antenna Design for Miniature Receivers," *IEEE Transactions on Antennas and Propagation*, pp. 528-530, July 1977.
3. Felix, R., *High Frequency Direction Finding: Errors, Algorithms, and OUTBOARD*, Master's Thesis, Naval Postgraduate School, Monterey, California, October 1982.
4. PATCH Code User's Manual, SANDIA Report, SAND87-2991, May 1988.

INITIAL DISTRIBUTION LIST

		No. Copies
1.	Defense Technical Information Center Cameron Station Alexandria, VA 22304-6145	2
2.	Library, Code 052 Naval Postgraduate School Monterey, CA 93943-5002	2
3.	Director, Space and Electronic Combat Division (N64) Space and Electronic Warfare Directorate Chief of Naval Operations Washington, D.C. 20393-5220	1
4.	Chairman, Electronic Warfare Academic Group, Code EW Naval Postgraduate School Monterey, CA 93943-9528	1
5.	Professor David Jenn, Code EC/Jn Department of Electrical and Computer Engineering Naval Postgraduate School Monterey, CA 93943-	2
6.	Professor Jeffrey B. Knorr, Code EC/Ko Department of Electrical and Computer Engineering Naval Postgraduate School Monterey, CA 93943-	1
7.	Embassy of Greece Naval Attache 2228 Massachusetts Ave., N.W. Washington, D.C. 20008	2

8. Ioannis Partsalidis
13 Megaloupoleos Str.
Kallithea, 17675
Athens
Greece 4

9. Randy Ott, SWL
3900 Juan Tabo, N.E.
Suite 12
Albuguergue, N.M., 87111 1

10. Gerald Peake
2301 S. Jefferson Davis Hwy
Apt. 523
Arlington, VA 22202 1

11. Peter Li, Code 824
EM Technology and Systems
NRAD
San Diego, CA 92152-5000 1